Long-wavelength limit of the dynamical local-field factor and dynamical conductivity of a two-component plasma

H. Reinholz
The University of Western Australia, Department of Physics, Nedlands, WA 6907, Australia

R. Redmer, G. Röpke, and A. Wierling
University of Rostock, FB Physik, Universitätsplatz 1, 18051 Rostock, Germany

(Received 6 October 1999; revised manuscript received 26 June 2000)

A systematic approach to the optical conductivity is given within a dielectric function formalism. The response function as well as the dynamical local-field factor $G(\vec{k},\omega)$ of an electron-ion plasma can be expressed in terms of determinants of equilibrium correlation functions which allow for a perturbative treatment. The dynamical collision frequency $\nu(\omega)=-i\omega_{\rm pl}^2 G(0,\omega)/\omega$ for fully ionized weakly coupled plasmas is evaluated in the low-density limit. A renormalization function is given to describe the effects of higher moments of the distribution function, thus the Spitzer formula is reproduced in the static limit. The existence of the third moment sum rule can be shown analytically. Numerical calculations are presented for the dynamical conductivity of hydrogen plasmas at solar core conditions.

PACS number(s): 52.25.Mq, 05.30.Fk, 71.45.Gm

I. INTRODUCTION

For a charged particle system, the longitudinal dielectric function $\epsilon(\vec{k},\omega)$ contains important information about different physical properties. It can be directly related to the wave vector $(\vec{k})$ and frequency (ω) dependent conductivity $\sigma(\vec{k},\omega)$ describing transport phenomena via $\epsilon(\vec{k},\omega)=1+i\sigma(\vec{k},\omega)/(\epsilon_0\omega)$. In particular, optical properties such as the refraction index, absorption coefficient, reflectivity, and bremsstrahlung are obtained considering the long-wavelength limit of the dielectric function $\epsilon(0,\omega)$ or the dynamical conductivity $\sigma(0,\omega)=\sigma(\omega)$, respectively.

With the advent of high-intensity femtosecond lasers it became feasible to produce nonideal plasmas at high densities and temperatures in the laboratory. The reflectivity and opacity of such laser-produced plasmas have been determined in a number of experiments, see [1–4].

The static limit of the frequency-dependent conductivity is related to the dc conductivity $\sigma_{\rm dc}$,

$$\sigma_{\rm dc}=\lim_{\omega\to 0}\lim_{k\to 0} i\epsilon_0\omega[1-\epsilon(\vec{k},\omega)]. \tag{1}$$

Several approaches are known that evaluate $\sigma_{\rm dc}$ and $\epsilon(\vec{k},\omega)$, leading to results which do not always fulfill the relation (1). Our main interest is to show which approximations have to be performed in evaluating $\epsilon(\vec{k},\omega)$ for weakly coupled plasmas at arbitrary degeneracy so that standard results for $\sigma_{\rm dc}$ are also reproduced.

The dc conductivity of a fully ionized plasma in the nondegenerate, weak-coupling limit is given by the Spitzer formula [5]. To include higher-density effects, a systematic many-particle treatment can be applied [6]. Using a generalized version of the linear-response theory [7,8], the connection to methods derived from kinetic equations [5,9–11] can easily be shown within the binary collision approximation. In contrast to the Kubo formula, expressions occurring in that generalized linear-response theory are of the type of force-force correlation functions and seem to be more appropriate for applying perturbation expansions for the dc conductivity. As a result, rigorous virial expansions have been given for the low-density limit [7,12]. A recent review considering general transport processes in dense plasmas is found in [13].

On the other hand, the dielectric function of a charged-particle system at finite frequencies can be obtained from a perturbation expansion of the Kubo formula [14], see also [15]. The dynamical conductivity of hot dense plasmas was investigated by different groups, see [16–18], starting from a Ziman formula [19] which was generalized for finite frequencies. Experimental data for metallic vapors at high densities [20], for a recent review see [21], or for the electrical resistivity of dense, laser pulse heated aluminum [22] are described successfully.

However, there exist parameter values corresponding to nondegenerate, weakly nonideal plasmas where the dc limit of the dynamical conductivity should be described by the Spitzer formula. The objective of this paper is to give a more general approach which refers also to fully ionized plasmas at low densities and high temperatures where the Spitzer formula and its improvements are applicable. For this case, expressions will be given for the dynamical conductivity. A renormalization factor is introduced to describe the effect of higher moments of the distribution function on the optical conductivity.

We follow the general treatment [23–26] given recently which bridges between the dielectric function and the dc conductivity. The main ingredient of the generalized linear-response theory [27] is a set of relevant observables which was introduced in correspondence to moments of the distribution function. In the present paper we elaborate the application of this approach to the dynamical response of a charged-particle system. Our objective is to show the level of approximation for the dynamical conductivity which is necessary in order to reproduce advanced treatments of the dc

conductivity, such as dynamical screening and inclusion of strong collisions, for fully ionized plasmas in the limit of small coupling parameters.

In the following, we consider a nonrelativistic charged-particle system with components c (mass m_c, charge e_c, spin s_c) described by the Hamiltonian

$$H=\sum_{p,c} E_p^c a_{p,c}^\dagger a_{p,c} + \frac{1}{2}\sum_{pp'q,cc'} V_{cc'}(q) a_{p-q,c}^\dagger a_{p'+q,c'}^\dagger a_{p',c'} a_{p,c}. \quad (2)$$

$E_p^c=\hbar^2 p^2/(2m_c)$ is the kinetic energy, $V_{cc'}(q)=e_c e_{c'}/(\epsilon_0 \Omega_0 q^2)$ the Coulomb interaction, Ω_0 the normalization volume, and $a_{p,c}^\dagger$ denotes the creation operator of a particle of component c with momentum $\hbar\vec{p}$. In particular, we will restrict ourselves to a two-component (hydrogen) plasma consisting of electrons and ions (protons) so that $c=e,i$. The spin variable will be included in the index c, and spin summations are performed in the final expressions. As an example, fully ionized hydrogen plasma is considered.

The paper is organized as follows: In Sec. II general expressions are given for the dynamical local-field factor and the dynamical collision frequency in terms of equilibrium correlation functions, which allow for a perturbative treatment. In Sec. III we consider the long-wavelength limit. Going beyond the Born approximation, partial summations are performed describing dynamical screening and strong collisions so that results for the dynamical conductivity match with results for the dc conductivity. Numerical results are presented for hydrogen plasmas at solar core conditions and sum rules are checked. In Sec. IV the convergence of the different collision terms and the inclusion of higher moments of the distribution function are discussed.

II. LINEAR-RESPONSE APPROACH FOR THE DIELECTRIC FUNCTION

A. Dynamical local-field factor and Drude formula

The calculation of the longitudinal dielectric function

$$\epsilon(\vec{k},\omega)=1-\frac{1}{\epsilon_0 k^2}\Pi(\vec{k},\omega) \quad (3)$$

for a charged fermion system, Eq. (2), in the lowest order with respect to the interaction gives the random-phase approximation (RPA) [28,29] for the polarization function $\Pi(\vec{k},\omega)$,

$$\Pi^{\mathrm{RPA}}(\vec{k},\omega)=\frac{1}{\Omega_0}\sum_{p,c} e_c^2 \frac{f_{p+k/2}^c - f_{p-k/2}^c}{\Delta E_{p,k}^c - \hbar(\omega+i\eta)}, \quad (4)$$

with $\Delta E_{p,k}^c = E_{p+k/2}^c - E_{p-k/2}^c = \hbar^2 \vec{k}\cdot\vec{p}/m_c$. Here, $f_p^c=[\exp(\beta E_p^c - \beta\mu_c)+1]^{-1}$ denotes the Fermi distribution function, $\beta=1/(k_B T)$ the inverse temperature, and μ_c the chemical potential of species c. The limit $\eta\to 0$ has to be taken after the thermodynamic limit.

Taking into account interaction processes, improvements of the RPA have been discussed extensively. A simple empirical approach to include scattering processes between particles and describe the optical conductivity is the frequently used Drude model (see, e.g., Ref. [14]) $\sigma(\omega)=\epsilon_0\omega_{\mathrm{pl}}^2/(-i\omega+\tau^{-1})$ with a relaxation time τ and the plasma frequency $\omega_{\mathrm{pl}}=[\Sigma_c e_c^2 n_c/(\epsilon_0 m_c)]^{1/2}$.

A more systematic approach is possible by introducing a dynamical local-field factor $G(\vec{k},\omega)$ [30] according to

$$\Pi(\vec{k},\omega)=\Pi^{\mathrm{RPA}}(\vec{k},\omega)/[1+G(\vec{k},\omega)\Pi^{\mathrm{RPA}}(\vec{k},\omega)/(\epsilon_0 k^2)].$$

Different approximative methods to determine $G(\vec{k},\omega)$ have been developed such as perturbation expansions [31], the parametrization of the dielectric function via sum rules [32,33], or a time-dependent mean-field theory [34]. A quantum statistical approach to the dynamical local-field factors at finite temperatures and arbitrary degeneracy was given by the authors in [25]. Using the relation

$$G(\vec{k},\omega)=\epsilon_0 k^2\left[\frac{1}{\Pi(\vec{k},\omega)}-\frac{1}{\Pi^{\mathrm{RPA}}(\vec{k},\omega)}\right], \quad (5)$$

and performing a perturbation expansion for the inverse of the polarization function $\Pi^{-1}(\vec{k},\omega)$, which goes beyond first-order local-field corrections in order to include collisions, this approach allows the direct connection to the theory of conductivity.

Considering the local-field factor in the long-wavelength limit and taking into account the RPA result $\lim_{k\to 0}\Pi^{\mathrm{RPA}}(\vec{k},\omega)=\epsilon_0\omega_{\mathrm{pl}}^2 k^2/\omega^2$, we find a Drude-like expression for the optical conductivity

$$\sigma(\omega)=\frac{\epsilon_0\omega_{\mathrm{pl}}^2}{-i\omega[1+\omega_{\mathrm{pl}}^2\,\mathrm{Re}\,G(0,\omega)/\omega^2]+\tau^{-1}(\omega)} = \frac{\epsilon_0\omega_{\mathrm{pl}}^2}{-i[\omega+i\nu(\omega)]} \quad (6)$$

with a frequency-dependent relaxation time $\tau^{-1}(\omega)=\omega_{\mathrm{pl}}^2\,\mathrm{Im}\,G(0,\omega)/\omega$. Alternatively, we can introduce a complex dynamical collision frequency

$$\nu(\omega)=-i\frac{\omega_{\mathrm{pl}}^2}{\omega}G(0,\omega). \quad (7)$$

The dc conductivity should result in the limit $\omega\to 0$,

$$\sigma_{\mathrm{dc}}=\lim_{\omega\to 0}\frac{\epsilon_0\omega_{\mathrm{pl}}^2}{\nu(\omega)}=i\lim_{\omega\to 0}\frac{\epsilon_0\omega}{G(0,\omega)}. \quad (8)$$

Before discussing the perturbation expansion of these expressions, we point out that the consistency of a given approximation can be checked by the inspection of certain sum rules

$$\int_{-\infty}^{\infty}\frac{d\omega}{\pi}\omega^n\,\mathrm{Im}\,\epsilon^{\pm 1}(\vec{k},\omega+i0)=S_n^{(\pm)}(\vec{k}), \quad (9)$$

see, e.g., [14]. We will focus on the f sum rule $S_1^{(-)}(\vec{k})=-\omega_{\mathrm{pl}}^2$, the conductivity sum rule $S_1^{(+)}(\vec{k})=\omega_{\mathrm{pl}}^2$, and the

third-moment sum rule $S_3^{(-)}(\vec{k})$. The latter has to be a finite value which is related to quantities such as the mean kinetic energy. An important point is that the third-moment sum rule is not convergent for the empirical Drude model approximation, which is obtained from Eq. (6) if taking the relaxation time τ as independent of frequency.

B. Linear-response theory

Within linear-response theory the longitudinal and transverse part of the dielectric function can be expressed by equilibrium correlation functions. Both expressions become identical [14] in the long-wavelength limit in which we are interested. Having this in mind, the relations relevant for the longitudinal dielectric function are presented.

A generalized version of the linear-response theory has been given recently [27] leading to the following expression for the response function [23]:

$$\chi(\vec{k},\omega)=i\beta\Omega_0\frac{k^2}{\omega}\frac{1}{M(\vec{k},\omega)}, \tag{10}$$

with the inverse response function

$$M(\vec{k},\omega)=|M_{lm}(\vec{k},\omega)|\Bigg/\begin{vmatrix}0 & M_{0m}(\vec{k},\omega)\\ M_{l0}(\vec{k},\omega) & M_{lm}(\vec{k},\omega)\end{vmatrix}. \tag{11}$$

The matrix elements $M_{ij}(\vec{k},\omega)$ of the determinants are given by equilibrium correlation functions of an appropriately chosen set of quantum operators $\{A_1,A_2,\ldots,A_l,\ldots\}$ which allows us to represent the electrical current-density operator

$$\vec{J}_k^{\rm el}=\frac{1}{\Omega_0}\sum_{p,c}\frac{e_c}{m_c}\hbar\vec{p}\,n_{p,k}^c \tag{12}$$

as a linear combination thereof; $n_{p,k}^c=a_{p-k/2,c}^\dagger a_{p+k/2,c}$ is the Wigner density. We have

$$M_{0m}(\vec{k},\omega)=(\vec{J}_k^{\rm el};A_m),\quad M_{l0}(\vec{k},\omega)=(A_l;\vec{J}_k^{\rm el}). \tag{13}$$

The elements of the submatrix $M_{lm}(\vec{k},\omega)$ are given by matrix operations according to

$$M_{lm}(\vec{k},\omega)=-i\omega(A_l;A_m)-(\dot{A}_l;A_m)+\langle\dot{A}_l;\dot{A}_m\rangle_{\omega+i\eta}+\begin{vmatrix}0 & \langle\dot{A}_l;A_j\rangle_{\omega+i\eta}\\ \langle A_i;\dot{A}_m\rangle_{\omega+i\eta} & \langle A_i;A_j\rangle_{\omega+i\eta}\end{vmatrix}\Bigg/|\langle A_i;A_j\rangle_{\omega+i\eta}|. \tag{14}$$

The equilibrium correlation functions are

$$(A;B)=\frac{1}{\beta Z}\int_0^\beta d\tau\,{\rm Tr}\left[{\rm e}^{-\beta H+\beta\sum_c \mu_c N_c}A(-i\hbar\tau)B^\dagger\right]$$
$$=\frac{1}{\beta}\int_{-\infty}^{\infty}\frac{d\omega'}{\pi}\frac{1}{\omega'}{\rm Im}\,\mathcal{G}_{AB^\dagger}(\omega'+i\eta),$$

$$\langle A;B\rangle_z=\int_0^\infty dt\,{\rm e}^{izt}(A(t);B)$$
$$=\frac{i}{\beta}\int_{-\infty}^{\infty}\frac{d\omega'}{\pi}\frac{1}{z-\omega'}\frac{1}{\omega'}{\rm Im}\,\mathcal{G}_{AB^\dagger}(\omega'+i\eta), \tag{15}$$

and $\dot{A}=(i/\hbar)[H,A]$, $Z={\rm Tr}\ {\rm e}^{-\beta H+\beta\Sigma_c\mu_c N_c}$. As already mentioned above, the limit $\eta\to 0$ in $z=\omega+i\eta$ has to be taken after the thermodynamic limit. The thermodynamic Green functions are obtained from the analytical continuation of $\mathcal{G}_{AB^\dagger}(\omega_\mu)$. They are calculated below at the Matsubara frequencies ω_μ using perturbation theory represented by diagram techniques.

From the response function $\chi(\vec{k},\omega)$, the polarization function can be deduced by $\Pi(\vec{k},\omega)=\chi(\vec{k},\omega)/[1+\chi(\vec{k},\omega)/(\epsilon_0k^2)]$, and subsequently the dynamical local-field factors $G(\vec{k},\omega)$ are directly related to the inverse response function $M(\vec{k},\omega)$ according to

$$G(\vec{k},\omega)=-i\frac{\epsilon_0\omega}{\beta\Omega_0}M(\vec{k},\omega)-\epsilon_0k^2\frac{1}{\Pi^{\rm RPA}(\vec{k},\omega)}+1. \tag{16}$$

To evaluate the general expression (11) for $M(\vec{k},\omega)$ the set of quantum operators $\{A_l\}$ needs to be specified. They define the rank of the matrices in Eq. (11). Following the framework known from standard transport theory [5] such as the Chapman-Enskog [9] or the Grad method [10] for the dc conductivity, the set of quantum operators $\{A_l\}$ is chosen as moments of the single-particle distribution function of each component of the system [8,23] taking

$$\{A_l\}\to\vec{P}_{k,n}^c=\sum_p\hbar\vec{p}\,(\beta E_p^c)^n n_{p,k}^c. \tag{17}$$

The first moments ($n=0;c=e,i$) are the momentum operators of the corresponding species. The electrical current-density operator (12) can easily be expressed as a linear combination of these observables. The second moments ($n=1$) are relevant in connection with the thermopower and thermal conductivity since they describe the current operators of the kinetic energy, see [8].

The approach by Eqs. (10)–(14) and (17) has been investigated in [23,24] with the current-density operator $\vec{J}_k^e=e_e\vec{P}_{k,0}^e/(m_e\Omega_0)$ of the electron system as the only considered relevant observable. The correlation functions were evaluated in the Born approximation. Before discussing the more general case in Sec. IV, we consider the first-moment

approach given by $\{A_l\}\to\{\vec{J}^e_k,\vec{J}^i_k\}$ in Sec. III. Within this choice of relevant observables, we obtain according to Eq. (14) the following expression for the ratio of determinants in $M(\vec{k},\omega)$, Eq. (11):

$$M_{JJ}(\vec{k},\omega)=-\frac{1}{\langle\vec{J}^{\rm el}_k;\vec{J}^{\rm el}_k\rangle_{\omega+i\eta}} \tag{18}$$

$$=-\frac{1}{(\vec{J}^{\rm el}_k;\vec{J}^{\rm el}_k)^2}\Bigg[-i\omega(\vec{J}^{\rm el}_k;\vec{J}^{\rm el}_k)+\langle\dot{\vec{J}}^{\rm el}_k;\dot{\vec{J}}^{\rm el}_k\rangle_{\omega+i\eta}-\frac{\langle\dot{\vec{J}}^{\rm el}_k;\vec{J}^{\rm el}_k\rangle_{\omega+i\eta}\langle\vec{J}^{\rm el}_k;\dot{\vec{J}}^{\rm el}_k\rangle_{\omega+i\eta}}{\langle\vec{J}^{\rm el}_k;\vec{J}^{\rm el}_k\rangle_{\omega+i\eta}}\Bigg]. \tag{19}$$

The first relation, which is obtained after partial integration [23], shows the coincidence with the Kubo formula. In contrast to the current-current correlation function itself, the inverse response function $M_{JJ}(\vec{k},\omega)$ can be expanded in perturbation theory avoiding singularities at zero wave vector, appearing otherwise already in the lowest order.

It can be shown by formal manipulations [35] that the results for the physical quantities given above are independent of the choice made for the set of quantum operators $\{A_l\}$ as long as the correlation functions are evaluated rigorously (and the limit $\eta\to0$ is performed in the final expressions). However, finite-order perturbation theory will lead to different results, depending on the choice of quantum operators $\{A_l\}$. In this context, the relation to the Kubo formula [6,14] has been discussed before in earlier papers [7,23].

C. Perturbation expansion of correlation functions

Having specified the set of quantum operators $\{A_l\}$ as $\{\vec{J}^e_k,\vec{J}^i_k\}$, we have to evaluate equilibrium correlation functions, Eq. (15), in order to find general expressions for the dynamical local-field factor $G(\vec{k},\omega)$, Eq. (16), and the related quantities $\chi(\vec{k},\omega),\Pi(\vec{k},\omega),\sigma(\vec{k},\omega)$.

The correlation function $(\vec{J}^c_k;\vec{J}^{c'}_k)$ contained in $(\vec{J}^{\rm el}_k;\vec{J}^{\rm el}_k)$ can be related to the commutator of position operator and operator of linear momentum (cf. [7]). With the particle density n_c we find the exact relations

$$(\vec{J}^c_k;\vec{J}^{c'}_k)=\delta_{cc'}\frac{e_c^2n_c}{m_c\beta\Omega_0}\quad\text{and}\quad(\vec{J}^{\rm el}_k;\vec{J}^{\rm el}_k)=\frac{\epsilon_0\omega_{\rm pl}^2}{\beta\Omega_0}. \tag{20}$$

The current-current correlation function occurring in the inverse response function $M_{JJ}(\vec{k},\omega)$, Eqs. (18) or (19), reads

$$\langle\vec{J}^c_k;\vec{J}^{c'}_k\rangle_{\omega+i\eta}=\frac{\hbar^2}{\Omega_0^2}\frac{e_ce_{c'}}{m_cm_{c'}}\sum_{pp'}p_zp'_z\langle n^c_{p,k};n^{c'}_{p',k}\rangle_{\omega+i\eta}. \tag{21}$$

The wave vector $\vec{k}=k\vec{e}_z$ is taken in the z direction and the system is considered to be isotropic. Further correlation functions arise where the particle current operators $\vec{J}^c_k$ are replaced by time derivatives (''forces'') $\dot{\vec{J}}^c_k$. Applying the commutator relation of the Hamiltonian with the current operators, Eq. (12), we arrive at expressions containing

$$\dot{n}^c_{p,k}=\frac{i}{\hbar}[H,n^c_{p,k}]=-\frac{ik}{m_c}\hbar p_zn^c_{p,k}+v^c_{p,k},$$

$$v^c_{p,k}=\frac{i}{\hbar}\sum_{p'qpd}V_{cd}(q)\{\delta^-_{p,p-q/2}-\delta^-_{p,p+q/2}\}\times a^{\dagger}_{\overline{p-k/2-q/2},c}a^{\dagger}_{p'+q/2,d}a_{p'-q/2,d}a^-_{p+k/2+q/2,c}. \tag{22}$$

Due to the potential-dependent part $v^c_{p,k}$ higher-order correlation functions will occur.

Let us now analyze the perturbation expansion of the expression (19) with respect to the coupling parameter e^2 [36]. In lowest order with respect to e^2 [37] we have $M^{(0)}_{JJ}(\vec{k},\omega)=i\beta\Omega_0k^2/[\omega\Pi^{\rm RPA}(\vec{k},\omega)]$ and subsequently $G^{(0)}(0,\omega)=0$ since the last term in Eq. (16) contributes in next order only. Notice that contributions in the lowest order arise from $\dot{\vec{J}}^{\rm el}_k$ which are produced from the kinetic part of $\dot{n}^c_{p,k}$, Eq. (22), not from the interaction part $v^c_{p,k}$.

In the next order of perturbation expansion, additional diagrams have to be considered adding one interaction line. The corresponding dynamical local-field factor which is related to quantum effects is given in Appendix A 1. It does not contribute to optical conductivities in the long-wavelength limit $k\to0$. Expanding the last brackets in Eq. (A2) in this limit shows that the first-order expression is $\propto k^2$ [24,26] and $\lim_{k\to0}M^{(1)}(\vec{k},\omega)=0$.

In order to allow for the inclusion of collisions which are of importance to obtain optical conductivities, we consider the second order of perturbation expansion $M^{(2)}(\vec{k},\omega)$. Some general expressions are given in Appendix A 1. Here we focus on the long-wavelength limit, where the local-field factor $G(0,\omega)$, Eq. (16), vanishes up to first order as discussed above. According to the long-wavelength limit of Eq. (A6) the force-force correlation function in Eq. (19),

$$\langle\dot{\vec{J}}^{\rm el}_0;\dot{\vec{J}}^{\rm el}_0\rangle_{\omega+i\eta}=\frac{\hbar^2}{\Omega_0^2}\sum_{pp',cc'}\frac{e_ce_{c'}}{m_cm_{c'}}p_zp'_z\lim_{k\to0}\langle v^c_{p,k};v^{c'}_{p',k}\rangle_{\omega+i\eta} \tag{23}$$

is of the order e^6. The last term in Eq. (19) contains correlation functions $\langle\vec{J}^{\rm el}_k;\dot{\vec{J}}^{\rm el}_k\rangle_{\omega+i\eta},\langle\dot{\vec{J}}^{\rm el}_k;\dot{\vec{J}}^{\rm el}_k\rangle_{\omega+i\eta}$ also being of the order e^6. This can be shown by diagram expansions or, more directly, making use of partial integration and the fact that due to the Kubo identity $(A;\dot{A})=i\langle[A,A]\rangle/(\hbar\beta)=0$ so that $\langle\vec{J}^{\rm el}_0;\dot{\vec{J}}^{\rm el}_0\rangle_z=(1/z)\langle\dot{\vec{J}}^{\rm el}_0;\dot{\vec{J}}^{\rm el}_0\rangle_z$, which is at least of the order e^6. In contrast, the correlation function $\langle\vec{J}^{\rm el}_0;\vec{J}^{\rm el}_0\rangle_{\omega+i\eta}$ is of the order e^2, cf. the RPA result for the polarization function $\Pi^{\rm RPA}(0,\omega)=\epsilon_0\omega_{\rm pl}^2k^2/\omega^2$. All together, the last contribution in Eq. (19) is of higher order (e^{10}) compared with $\langle\dot{\vec{J}}^{\rm el}_0;\dot{\vec{J}}^{\rm el}_0\rangle_{\omega+i\eta}$. Therefore, the second-order contribution to the dynamical local-field factor in the long-wavelength limit is

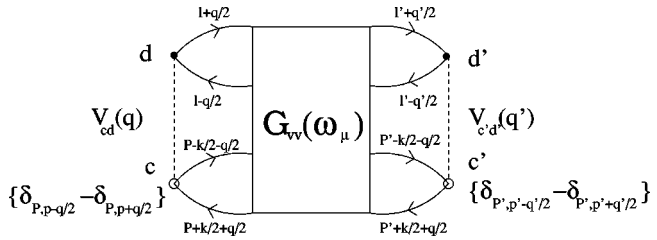

FIG. 1. Representation of the Green function $\mathcal{G}_{vv}(\omega_\mu)$ by Feynman diagrams.

$$G^{(2)}(0,\omega)=i\frac{\omega}{\omega_{\rm pl}^2}\nu^{(2)}(\omega)=i\omega\frac{\beta\Omega_0}{\epsilon_0\omega_{\rm pl}^4}\langle\dot{\vec{J}}_0^{\rm el};\dot{\vec{J}}_0^{\rm el}\rangle_{\omega+i\eta}^{(2)}. \tag{24}$$

III. FREQUENCY-DEPENDENT CONDUCTIVITY

In order to calculate the dynamical collision frequency, see Eqs. (23) and (24), the correlation function

$$\begin{aligned}\langle v_{p,k}^{c};v_{p',k}^{c'}\rangle_{\omega+i\eta}&=\frac{1}{\hbar^2}\sum_{dd'qq'll'\overline{pp'}}V_{cd}(q)V_{c'd'}(q')\\&\times\{\delta_{\overline{p},p-q/2}-\delta_{\overline{p},p+q/2}\}\\&\times\{\delta_{\overline{p'},p'-q'/2}-\delta_{\overline{p'},p'+q'/2}\}\\&\times\langle a^{\dagger}_{\overline{p-k/2-q/2},c}a^{\dagger}_{l+q/2,d}a_{l-q/2,d}\\&\times a_{\overline{p+k/2+q/2},c};a^{\dagger}_{\overline{p'-k/2-q'/2},c'}a^{\dagger}_{l'+q'/2,d'}\\&\times a_{l'-q'/2,d'}a_{\overline{p'+k/2+q'/2},c'}\rangle_{\omega+i\eta}\end{aligned} \tag{25}$$

will be evaluated using the relation (15) to the corresponding four-particle Green function $\mathcal{G}_{vv}(\omega_\mu)$ (the single-particle variables are omitted), see Fig. 1. Details are presented in Appendixes A 2–A 4.

In the lowest approximation with respect to the interaction (Born approximation, see Fig. 2 and Appendix A 2), we find according to Eq. (A8) the complex dynamical collision frequency

$$\begin{aligned}\nu^{\rm Born}(\omega)=i\frac{4\hbar}{\Omega_0 n\mu}\sum_{pp'q}&\frac{e^{\beta(\Delta E^i_{p',q}-\Delta E^e_{p,q})}-1}{\Delta E^i_{p',q}-\Delta E^e_{p,q}}q_z^2V_{ei}^2(q)\\&\times\frac{f^i_{p'+q/2}(1-f^i_{p'-q/2})f^e_{p-q/2}(1-f^e_{p+q/2})}{\hbar(\omega+i\eta)+\Delta E^i_{p',q}-\Delta E^e_{p,q}}.\end{aligned} \tag{26}$$

The reduced mass $\mu^{-1}=m_e^{-1}+m_i^{-1}$ follows from the sum over the species with $e_e=-e_i=e$, $n_e=n_i=n$. The factor 4 is due to the summation over spin variables, $s_e=s_i=1/2$. For $\Delta E^c_{p,q}$ see Eq. (4). Due to momentum conservation there is no contribution from the interactions between particles of the same component in this one-moment approach.

The corresponding dc conductivity, Eq. (8), is applicable to short-range interactions. However, $\sigma_{\rm dc}^{\rm Born}=\epsilon_0\omega_{\rm pl}^2/\nu^{\rm Born}(0)$ cannot be considered as a correct expression for the dc conductivity of a Coulomb system, Eq. (2), for different reasons: Due to the long-range character of the Coulomb interaction, the Born approximation is divergent. Screening has to be taken into account. Strong collisions may occur so that a T-matrix approach is necessary. This way, the correct Coulomb logarithm for the low-density limit will be obtained performing the corresponding partial summations. Furthermore, to reproduce the correct prefactor of the Spitzer formula, which is valid in the nondegenerate, low-density limit, higher moments of the distribution function, Eq. (17), need to be taken into account.

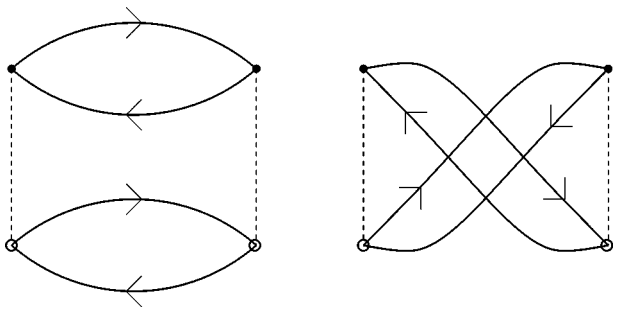

FIG. 2. Green function $\mathcal{G}_{vv}(\omega_\mu)$ in the Born approximation.

These arguments, well known from the evaluation of the dc conductivity of a plasma, see [7], apply also to the more general case of the dynamical conductivity. We reconsider the evaluation of

$$\nu(\omega)\approx\frac{\beta\hbar^2}{\Omega_0\epsilon_0\omega_{\rm pl}^2}\sum_{pp',cc'}\frac{e_ce_{c'}}{m_cm_{c'}}p_zp'_z\lim_{k\to0}\langle v_{p,k}^{c};v_{p',k}^{c'}\rangle_{\omega+i\eta} \tag{27}$$

beyond Born approximation by including higher-order terms of the perturbation expansion. In particular, we introduce the dynamically screened interaction by summation over ring diagrams, and consider the Born approximation with respect to the screened interaction. Furthermore, performing the partial summation over the ladder diagrams, the T-matrix is introduced describing binary collisions in the correct way. To include the effects of higher densities, further diagrams can be included such as self-energy corrections and three-vertex terms. However, in the present work we consider only the low-density limit of the dynamical conductivity, where self-energy corrections and three-vertex terms can be dropped, cf. the arguments given in the case of the dc conductivity in [7].

A. Dynamical screening

1. Summation of ring diagrams

Comparing with the simple Born approximation, ring diagrams are produced replacing a simple loop by a chain of loops, see Fig. 3. More generally, the summation of all loop diagrams is included by introducing the dynamically screened potential $V^s_{cc'}(q,z)=V_{cc'}(q)/\epsilon(q,z)$, which will be represented by a wavy line. The screened Born approximation is given by the diagrams for $\mathcal{G}_{vv}(\omega_\mu)$ shown in Fig. 4, see also [7]. When evaluating the Green function, which is detailed in Appendix A 3, we use the spectral representation of the screened potential, see, e.g. [38],

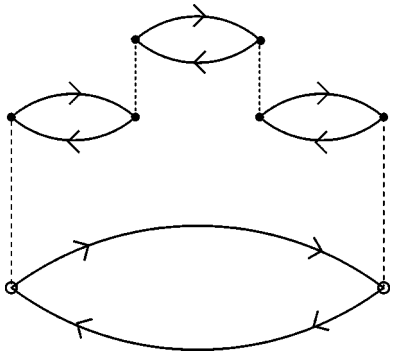

FIG. 3. Example of a contribution to the Green function $\mathcal{G}_{vv}(\omega_\mu)$ in a dynamically screened approximation.

$$V^s_{cc'}(q,\omega_\nu)=V_{cc'}(q)+V_{cc'}(q)\int\frac{d\omega}{\pi}\frac{\mathrm{Im}\,\epsilon^{-1}(q,\omega+i0)}{\omega-\omega_\nu}. \tag{28}$$

Using the relation (3), the inverse dielectric function can be expressed by the polarization function

$$\mathrm{Im}\,\epsilon^{-1}(q,\omega+i0)=\frac{\mathrm{Im}\,\Pi(q,\omega+i0)}{\epsilon_0 q^2|\epsilon(q,\omega)|^2}. \tag{29}$$

Since we are interested in the low-density limit we can take the polarization function and the dielectric function in the RPA limit, Eq. (4). As well known [14], the dynamical structure factor corresponding to this RPA dielectric function describes excitations in a two-component plasma including a slightly renormalized electron plasma frequency and an ion-acoustic plasma mode. Utilizing

$$\frac{1}{\epsilon_0 q^2}\mathrm{Im}\,\Pi^{\mathrm{RPA}}(q,\omega+i0)$$

$$=-\pi\sum_{pc}V_{cc}(q)[f^c_{p+q/2}-f^c_{p-q/2}]\delta(\Delta E^c_{p,q}-\hbar\omega), \tag{30}$$

the dynamical collision frequency, Eq. (27), in the screened Born approximation is obtained, see Appendix A 3,

$$\nu^{\mathrm{LB}}(\omega)=i\frac{4\hbar\mu}{\Omega_0 n}\sum_{pp'q}\frac{e^{\beta(\Delta E^i_{p',q}-\Delta E^e_{p,q})}-1}{\Delta E^i_{p',q}-\Delta E^e_{p,q}}q_z^2V^2_{ei}(q)$$
$$\times\frac{f^e_{p-q/2}(1-f^e_{p+q/2})f^i_{p'+q/2}(1-f^i_{p'-q/2})}{\hbar(\omega+i\eta)+\Delta E^i_{p',q}-\Delta E^e_{p,q}}$$
$$\times\left[\frac{1}{m_e|\epsilon_{\mathrm{RPA}}(q,\Delta E^i_{p',q}/\hbar)|}\right.$$
$$\left.+\frac{1}{m_i|\epsilon_{\mathrm{RPA}}(q,\Delta E^e_{p,q}/\hbar)|}\right]^2. \tag{31}$$

The expression (31) has the same structure as the Born approximation, Eq. (26), except the bare Coulomb interaction is screened by the full RPA expression of the dielectric function.

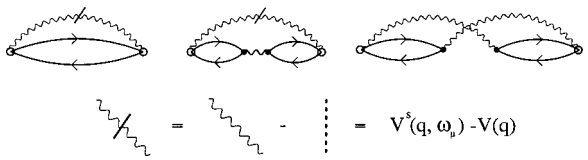

FIG. 4. Contributions to the Green function $\mathcal{G}_{vv}(\omega_\mu)$ in a dynamically screened Born approximation.

In adiabatic approximation $\lim(m_i/m_e)\to\infty$, the electrons are considered to scatter from ions at positions $\vec{R}_j$. We find the following expression for the dynamical collision frequency:

$$\nu^{\mathrm{LB}}(\omega)=-i\frac{2\hbar n_i}{m_e n_e}\sum_{pq}\frac{V^2_{ei}(q)S_i(q)}{|\epsilon_{\mathrm{RPA},e}(q,\Delta E^e_{p,q}/\hbar)|^2}q_z^2$$
$$\times\frac{f^e_{p+q/2}-f^e_{p-q/2}}{\Delta E^e_{p,q}-\hbar(\omega+i\eta)}\frac{1}{\Delta E^e_{p,q}}$$
$$=i\frac{\epsilon_0 n_i\Omega_0^2}{6\pi^2e^2n_em_e}\int_0^\infty dq\,q^6V^2_{ei}(q)S_i(q)\frac{1}{\omega}[\epsilon^{-1}_{\mathrm{RPA},e}(q,\omega)$$
$$-\epsilon^{-1}_{\mathrm{RPA},e}(q,0)], \tag{32}$$

where the ion distribution is taken into account by the ionic structure factor $S_i(q)=\Sigma_{jl}\exp[i\vec{q}\cdot(\vec{R}_j-\vec{R}_l)]/(n_i\Omega_0)$ on the static level, replacing the ionic contribution to the dielectric function. The remaining $\epsilon_{\mathrm{RPA},e}(q,\omega)$ is determined only by the electron component of the plasma. Evaluating this adiabatic expression for a classical plasma (nondegenerate case) we find an expression as given before by Bekefi [39] whereas the zero-temperature limit for a simple metal was considered by Hopfield [40]. Splitting the dynamical collision frequency into real and imaginary parts leads to a Drude-like expression (6) for the electrical conductivity with a frequency-dependent relaxation time for a dynamically screened Coulomb potential.

In the zero-frequency limit, the imaginary part of the collision frequency vanishes. The inverse relaxation time, derived from Eq. (31),

$$\frac{1}{\tau^{\mathrm{LB}}(0)}=\nu^{\mathrm{LB}}(0)$$
$$=-\frac{\hbar}{\Omega_0 n\mu}4\sum_{pp'q}q_z^2\frac{V^2_{ei}(q)}{|\epsilon_{\mathrm{RPA}}(q,\Delta E^e_{p,q})|^2}f^e_{p-q/2}$$
$$\times(1-f^e_{p+q/2})f^i_{p'+q/2}(1-f^i_{p'-q/2})$$
$$\times\delta(\Delta E^i_{p',q}-\Delta E^e_{p,q}), \tag{33}$$

coincides with the well-known Lenard-Balescu collision integral [41] and has been derived before within the linear-response theory in [7,42].

The Ziman formula [19] for the dc conductivity can be found from the adiabatic limit, Eq. (32),

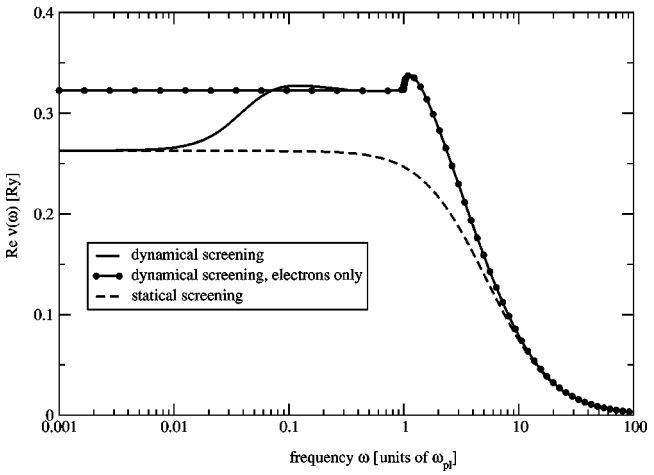

FIG. 5. Real part of the dynamical collision frequency ν^{LB} as a function of frequency ω for a classical electron and a two-component plasma at solar core conditions in comparison to the statically screened Born approximation.

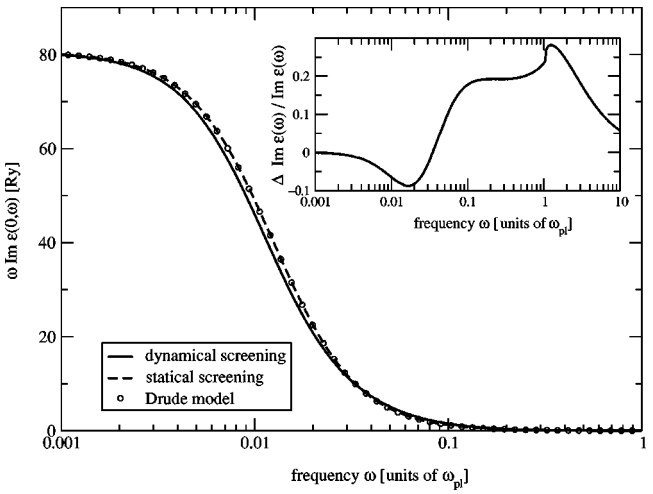

FIG. 6. Dynamical conductivity σ^{LB} as a function of frequency ω for a classical two-component plasma at solar core conditions in comparison to the statically screened Born approximation.

$$\sigma_{\mathrm{dc}}^{\mathrm{Ziman}}=\frac{\epsilon_0\omega_{\mathrm{pl}}^2}{\nu^{\mathrm{Ziman}}(0)}$$
$$=\frac{12\pi^3\hbar^3e^2n_e^2}{\Omega_0^2m_e^2n_i}\left[\int_0^\infty dq\,q^3\frac{V_{ei}^2(q)S_i(q)}{|\epsilon_{\mathrm{RPA},e}(q,0)|^2}f_{q/2}^e\right]^{-1}. \tag{34}$$

The inclusion of ion dynamics considering the dynamical ionic structure factor is straightforward and coincides with the expression (33) for the two-component system if the relation between the dynamic structure factor and the dielectric function is taken into account. In this case, the dc conductivity is influenced by dynamical screening, and the frequency argument of the dielectric function is an energy-dependent variable. The connection between the Ziman formula and the Lenard-Balescu result was also in investigated in [43].

With Eq. (31) and its adiabatic limit, Eq. (32), we derived a generalized Drude formula (6) for the optical conductivity. This result applies to the low-density limit. The dynamical conductivity from the first-moment approach in screened Born approximation, Eq. (32), has also been applied to higher densities, see [16–18,20,22]. However, instead of the dynamically screened Coulomb potential a pseudopotential has been considered. The ionic structure factor was evaluated by standard methods from the theory of liquids. Density effects were included into the electronic part of the dielectric function describing the screening of the electron-ion interaction taking into account local-field factors.

2. Numerical results

The evaluation of the complex collision frequency, Eq. (31), has been performed for a hydrogen plasma at the conditions of the solar core, i.e., $T=96.15$ Ry, $n_e=n_i=n=8.9a_B^{-3}$. This is a weakly coupled plasma, $\Gamma=e^2(4\pi n/3)^{1/3}/(4\pi\epsilon_0k_BT)=0.069$, which is not strongly degenerate, $\Theta=2m_ek_BT(3\pi^2n)^{-2/3}/\hbar^2=2.34$. The screening parameter is $\kappa_D=(\beta\Sigma_ce_c^2n_c/\epsilon_0)^{1/2}=2.15/a_B$ and the plasma frequency $\hbar\omega_{\mathrm{pl}}=21.15$ Ry. In Fig. 5 the real part of the collision frequency, Eq. (31), is compared with the collision frequency of the statically screened Born approximation using $\epsilon(q,0)=1+\kappa_D^2/q^2$ in Eq. (31). From Fig. 5 we deduce that the dynamical collision frequency coincides with a static description at small frequencies. The high-frequency behavior is also in agreement with the static treatment. In between, a pronounced effect is seen due to the inclusion of dynamical screening. In particular, a peak appears due to the excitation of plasmons, cf. Refs. [40,44].

The corresponding calculations for the imaginary part of the dielectric function, Eq. (6), are shown in Fig. 6. The static evaluation almost coincides with the Drude result, where the collision frequency is approximated by the zero-frequency relaxation time. Differences are obtained by taking into account dynamical screening. The inset shows the deviation when using a statically screened approximation in comparison to the dynamical evaluation. Of particular interest is the plasmon peak occurring in the response function $\mathrm{Im}\,\epsilon^{-1}(\vec{k},\omega)$ and its dispersion as shown in Fig. 7, see also

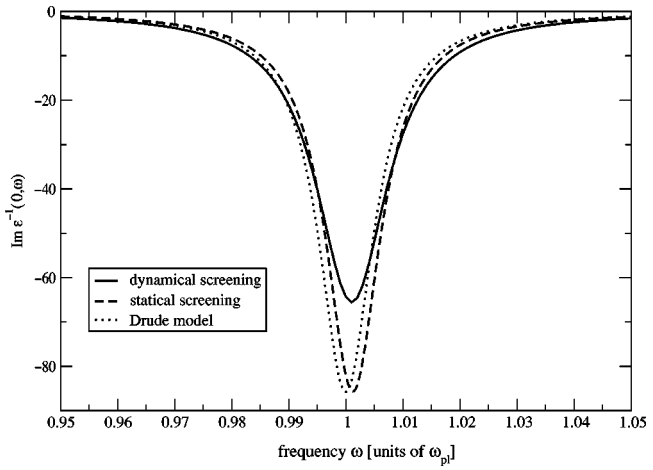

FIG. 7. Imaginary part of the inverse dielectric function as a function of frequency ω for a classical two-component plasma at solar core conditions in comparison to the statically screened Born approximation and the Drude model.

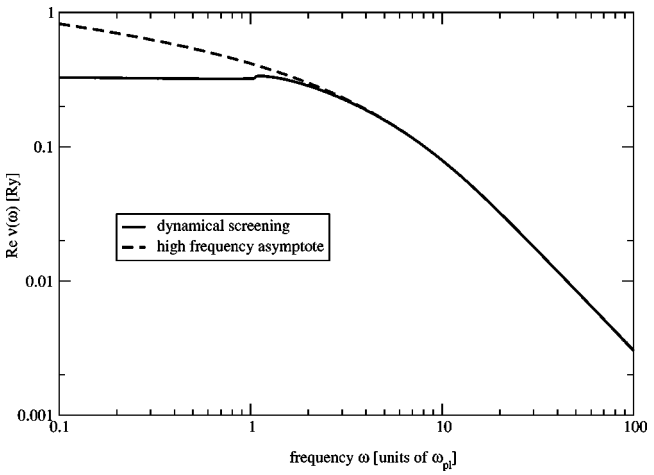

FIG. 8. High-frequency limit of the real part of the dynamical collision frequency ν^{LB} as a function of frequency ω for a classical two-component plasma at solar core conditions.

[25]. While the Drude model shows the plasmon peak at the plasma frequency the more consistent treatment of the dielectric function leads to a shift of the peak in comparison to the plasma frequency due to the imaginary part of the collision frequency. The dynamical screening broadens the plasmon peak and reduces the depth of the peak compared with the Drude model.

Note that the approximation of the dielectric function considered here obeys the Kramers-Kronig relation. Since the asymptotic form of the real part of the dielectric function is given by $\lim_{\omega\to\infty}\epsilon(0,\omega)=1-\omega_{\mathrm{pl}}^2/\omega^2+\cdots$, the first-moment sum rules (9) are fulfilled following the argument in Ref. [14]. This has also been checked numerically. To fulfill the first-moment sum rules, the account of the imaginary part of the collision frequency appears to be crucial. It emphasizes that an empirical improvement of the Drude formula introducing solely a frequency-dependent relaxation time does not obey sum rules, and thus it is not a consistent approximation.

The high-frequency behavior of the collision frequency is determined by the Born approximation only, Eq. (26), as derived in Appendix B. The imaginary part of the collision frequency is found to be proportional to $\omega^{-3/2}$. It ensures the existence of the third moment of the imaginary part of the dielectric function as required by the corresponding sum rule, Eq. (9). A comparison between the exact dynamical screening result and the high-frequency asymptote is shown in Fig. 8. The Born approximation given in Eq. (B5) coincides with the asymptote for frequencies down to about $4\omega_{\mathrm{pl}}$.

B. Strong collisions

1. Summation of ladder diagrams

Considering the dc conductivity of Coulomb systems, the collision integral in the Born approximation is divergent not only for small transfer momenta q, which is cured introducing the dynamically screened interaction as discussed above. As well known, see, e.g. [8,13], for large values of q the collision integral in the Born approximation is divergent if the classical limit is considered.

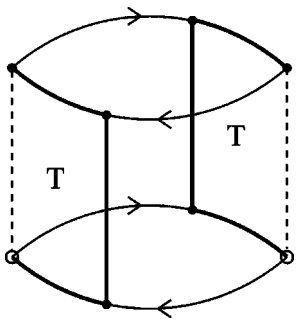

FIG. 9. Green function $\mathcal{G}_{vv}(\omega_\mu)$ in the ladder approximation.

This divergence is avoided if higher orders of the perturbation expansion are taken into account. The behavior for large values of q is determined by strong binary collisions which are accounted for by summing up the so-called ladder diagrams in the perturbation expansion, see Fig. 9 and Appendix A 4. In the quantum case, the divergence in the Born approximation for large values of q disappears, because the corresponding short-range part of the Coulomb potential is averaged out due to quantum effects. The typical length scale is the thermal wavelength. However, also in the quantum case the correct result in the low-density limit for the dc conductivity is only obtained after performing the sum over the ladder diagrams [7]. Therefore, it is necessary to take into account strong binary collisions in order to evaluate the dynamical collision frequency in the low-density limit.

We evaluate the correlation function, Eq. (27), in the limit $k\to 0$. The summation of ladder diagrams in the corresponding Matsubara Green function $\mathcal{G}_{vv}^{\mathrm{ladder}}(\omega_\mu)$ is shown in Appendix A 4 for arbitrary mass ratios m_i/m_e. In this section we consider the adiabatic limit $m_e/m_i\to 0$, thus

$$\nu^{\mathrm{ladder}}(\omega)=\frac{4\beta\hbar^2}{n_e m_e\Omega_0}\sum_{pp'} p_z p_z' \langle v^e_{p,0};v^e_{p',0}\rangle^{\mathrm{ladder}}_{\omega+i\eta}. \quad (35)$$

As already pointed out in the discussion of the Born approximation, because of the conservation of the total momentum only the interaction between electrons and ions will contribute. With Appendix A 4, Eq. (A15), we find in the binary collision approximation

$$\nu^{\mathrm{ladder}}(\omega)=\frac{i\hbar}{\Omega_0 n_e m_e}\sum_{nn'P}\frac{e^{\beta(E_{nP}-E_{n'P})}-1}{E_{nP}-E_{n'P}} \times\frac{g^{ei}(E_{nP})[1+g^{ei}(E_{n'P})]}{\hbar(\omega+i\eta)+E_{nP}-E_{n'P}}\left|\sum_{p_e,p_i,q}\psi^*_{n'P}(p_e,p_i) \times V(q)q_z\psi_{nP}(p_e+q,p_i-q)\right|^2 \quad (36)$$

with $\psi_{nP}(p_e,p_i)$ being the wave function, E_{nP} the energy eigenvalue for the two-particle state with center-of-mass momentum P and internal quantum number n, and $g^{ei}(E)=\{\exp[\beta(E-\mu_e-\mu_i)]-1\}^{-1}$ the Bose distribution function.

By introducing T matrices, the following expression can be found [see Appendix A 4, Eqs. (A20) and (A21)]:

$$\nu^{\rm ladder}(\omega)=\frac{i\hbar}{\Omega_0 m_e n_e}4\sum_{p_e p_i q}\frac{e^{\beta(E^{ei}_{p,0}-E^{ei}_{p,q})}-1}{\hbar(\omega+i\eta)+E^{ei}_{p,0}-E^{ei}_{p,q}}\frac{1}{E^{ei}_{p,0}-E^{ei}_{p,q}}f^e_{p_e}(1-f^e_{p_e+q})f^i_{p_i}(1-f^i_{p_i-q})\Bigg\{(p_{e,z}+q_z)T^-_{ei}(p_e,p_i;q;E^{ei}_{p,0})$$
$$-p_{e,z}T^-_{ei}(p_e,p_i;q;E^{ei}_{p,q})-\sum_{q'}(p_{e,z}+q'_z)T^-_{ei}(p_e,p_i;q';E^{ei}_{p,0})\left[\frac{1}{E^{ei}_{p,0}-E^{ei}_{p,q'}-i\hbar\eta}-\frac{1}{E^{ei}_{p,q}-E^{ei}_{p,q'}-i\hbar\eta}\right]$$
$$\times T^-_{ei}(p_e+q',p_i-q';-q'+q;E^{ei}_{p,q})\Bigg\}\Bigg\{(p_{e,z}+q_z)T^+_{ei}(p_e+q,p_i-q;-q;E^{ei}_{p,0})-p_{e,z}T^+_{ei}(p_e+q,p_i-q;$$
$$-q;E^{ei}_{p,q})+\sum_{q''}(p_{e,z}+q''_z)T^+_{ei}(p_e+q,p_i-q;-q+q'';E^{ei}_{p,q})\left[\frac{1}{E^{ei}_{p,q}-E^{ei}_{p,q''}+i\hbar\eta}-\frac{1}{E^{ei}_{p,0}-E^{ei}_{p,q''}+i\hbar\eta}\right]$$
$$\times T^+_{ei}(p_e+q'',p_i-q'';-q'';E^{ei}_{p,0})\Bigg\}, \tag{37}$$

where the abbreviations $T^{\pm}_{ei}(p_e,p_i;q;E)=T^{\pm}_{ei}(p_e,p_i;p_e+q,p_i-q;E)$ and $E^{ei}_{p,q}=E^e_{p_e+q}+E^i_{p_i-q}$ were used. The Fermi functions occurring in the T matrices such as $(1-f^e_{p_e}-f^i_{p_i})$ were neglected since we consider the nondegenerate case in the following. Equation (37) contains the half off-shell T matrices for the electron-ion scattering, where the energy coincides with either the incoming or the outgoing energy, respectively. In general,

$$T^{\pm}_{ei}(p_e,p_i;q;E)$$
$$=V_{ei}(q)+\sum_{q'}V_{ei}(q')\frac{1}{E-E^{ei}_{p,q'}\pm i\eta}$$
$$\times T^{\pm}_{ei}(p_e+q',p_i-q';-q'+q;E) \tag{38}$$

holds for arbitrary values of energy E.

From the complex dynamical collision frequency in ladder approximation follows $\sigma^{\rm ladder}_{\rm dc}=\epsilon_0\omega^2_{\rm pl}/\nu^{\rm ladder}(0)$ in the zero-frequency limit. From the general symmetry property rhs $(\omega)=[{\rm rhs}(-\omega)]^*$ of the right-hand side (rhs) of Eq. (37), we conclude that it must be real for $\omega=0$. Therefore, in the decomposition due to the Dirac identity $i/(\omega-\omega'+i\eta)=\pi\delta(\omega-\omega')+i\mathcal{P}/(\omega-\omega')$ only the δ function describing the conservation of kinetic energy gives a contribution. Then, products of two on-shell T matrices remain which can be expressed in terms of scattering phase shifts. The higher-order products of T matrices in Eq. (37) vanish because the difference in the square brackets is equal to zero. We obtain

$$\nu^{\rm ladder}(0)=\frac{\pi\hbar\beta}{\Omega_0 m_e n_e}4\sum_{p_e p_i q}q_z^2 f^e_{p_e}(1-f^e_{p_e+q})f^i_{p_i}(1-f^i_{p_i-q})$$
$$\times\delta(E^{ei}_{p,q}-E^{ei}_{p,0})T^-_{ei}(p_e,p_i;q;E^{ei}_{p,0})$$
$$\times T^+_{ei}(p_e+q,p_i-q;-q;E^{ei}_{p,0}). \tag{39}$$

In an adiabatic approximation, we perform the integration over p_i to give a factor $n_i\Omega_0$ and relate the product of the T matrices to the transport cross section $\mathcal{Q}^T_{ei}(k)=(4\pi/k^2)\Sigma^{\infty}_{l=0}(l+1)\sin^2[\delta^{ei}_{l+1}(k)-\delta^{ei}_l(k)]$, see Refs. [7,8,42], where $\delta^{ei}_l(k)$ are the scattering phase shifts. Taking the nondegenerate limit, we obtain

$$\nu^{\rm ladder}(0)=\frac{8}{3\sqrt{\pi}}\frac{\hbar n_i}{m_e}\left(\frac{\beta\hbar^2}{2m_e}\right)^{5/2}\int_0^{\infty}dk\,k^5 e^{-\beta\hbar^2k^2/(2m_e)}\mathcal{Q}^T_{ei}(k). \tag{40}$$

This way, the correct zero-frequency limit for the collision frequency is reproduced.

2. Numerical results

As above, we consider a hydrogen plasma at solar core conditions. In the following, we perform the evaluation of the expression (37) for an effective interaction potential, replacing the Coulomb potential by $V^{\rm eff}_{ei}(q)=-e^2/[\epsilon_0\Omega_0(q^2+\kappa^2_{\rm eff})]$, thus avoiding the divergences for small q. The effective screening parameter $\kappa_{\rm eff}$ was determined in such a way that the Coulomb logarithm obtained from the Lenard-Balescu collision term (33) for the dc conductivity coincides with the Coulomb logarithm obtained for the $V^{\rm eff}_{ei}(q)$ in the Born approximation so that $\kappa^2_{\rm eff}=1.47n\beta e^2/\epsilon_0$ [7,42]. This expression can be interpreted in such a way that the dynamical screening corresponds to an effective density $1.47n$ in between the electron density n and the density $2n$ of electrons and ions.

First, we consider the zero-frequency limit. The transport cross section $\mathcal{Q}^T_{ei}(k)$ becomes in quasiclassical approximation [7,8,42]

$$\mathcal{Q}^T_{ei}(k)=\frac{4\pi}{a_B^2k^4}\ln\left(0.681\frac{k^2a_B}{\kappa_{\rm eff}}\right), \tag{41}$$

where $a_B=4\pi\epsilon_0\hbar^2/(m_e e^2)$ is the Bohr radius. Performing the integral over k in Eq. (40) we find

$$\nu^{\rm ladder}(0)=\frac{4}{3}\sqrt{2\pi}\frac{n_i\beta^{3/2}e^4}{m_e^{1/2}(4\pi\epsilon_0)^2}L_{\rm ladder},$$
$$L_{\rm ladder}=\ln\left(0.765\frac{4\pi\epsilon_0}{\beta e^2\kappa_{\rm eff}}\right). \tag{42}$$

From this result, we obtain the low-density limit for the dc conductivity,

$$\sigma_{\rm dc}^{\rm ladder}=\frac{3}{4\sqrt{2\pi}}\frac{(4\pi\epsilon_0)^2}{\beta^{3/2}m_e^{1/2}e^2}\frac{n_e}{n_i}L_{\rm ladder}^{-1} \tag{43}$$

which should be compared with the Spitzer formula [5]

$$\sigma_{\rm dc}^{\rm Sp}=0.591\frac{(4\pi\epsilon_0)^2}{\beta^{3/2}m_e^{1/2}e^2}\frac{n_e}{n_i}L_{\rm Sp}^{-1}\,. \tag{44}$$

The Spitzer Coulomb logarithm $L_{\rm Sp}=\ln[(3/\sqrt{2})4\pi\epsilon_0/(\beta e^2\kappa_D)]$ coincides with the Coulomb logarithm $L_{\rm ladder}$ in the ladder approximation for the screened interaction potential up to an additive constant reflecting the different treatment of the screening of the Coulomb interaction. Compared with the statically screened Born approximation, where the Brooks-Herring Coulomb logarithm appears (cf. Ref. [7]), the dependence of the leading logarithmic term of the virial expansion on density and temperature has been changed. Despite the correct value for the Coulomb logarithm, obtained in the T matrix approach in leading order, the prefactor does not coincide with the Spitzer result. To obtain the correct prefactor one can consider higher moments of the single-particle distribution function as will be discussed in the following section.

After making the connection to the dc conductivity by considering the zero-frequency limit, we want to investigate the frequency dependence of the collision frequency, Eq. (37). The numerical method applied to evaluate the half off-shell T matrices is given in Appendix C. For the exploratory evaluation given here, the higher-order products of the T matrices occurring in Eq. (37) have been neglected. Using the relative momentum $\vec{p}_r=(m_i\vec{p}_e-m_e\vec{p}_i)/(m_e+m_i)\approx\vec{p}_e$ the partial wave decomposition of the T matrix reads

$$T^{\pm}(p_e,p_i;q;E)=\sum_{l=0}^{\infty}(2l+1)T_l^{\pm}(p_r,|\vec{p}_r+\vec{q}|;E)P_l(\cos\theta) \tag{45}$$

with the Legendre polynomials $P_l(\cos\theta)$, θ being the angle between $\vec{p}_r$ and $(\vec{p}_r+\vec{q})$. Insertion of Eq. (45) yields, after performing the integrals over the angular parts,

$$\begin{aligned}\mathrm{Re}\,\nu^{\rm ladder}(\omega)=&\frac{\beta\Omega_0^2}{3\pi^3\hbar}\int_0^\infty dp\,p^2\int_0^\infty dp'\,p'^2\frac{1-e^{-\beta\hbar\omega}}{\beta\hbar\omega}\\&\times\delta\left(p^2-p'^2+\frac{2m_e\omega}{\hbar}\right)f_p^e\sum_{l=0}^{\infty}(l+1)\\&\times[\{p'T_l^-(p,p';E_p^e)-pT_{l+1}^-(p,p';E_{p'}^e)\}\\&\times\{p'T_l^+(p',p;E_p^e)-pT_{l+1}^+(p',p;E_{p'}^e)\}\\&+\{pT_l^-(p,p';E_{p'}^e)-p'T_{l+1}^-(p,p';E_p^e)\}\\&\times\{pT_l^+(p',p;E_{p'}^e)-p'T_{l+1}^+(p',p;E_p^e)\}].\end{aligned} \tag{46}$$

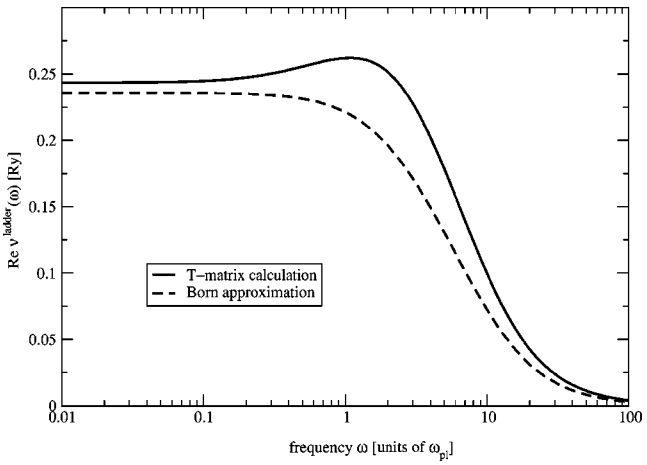

FIG. 10. Real part of the collision frequency $\nu^{\rm ladder}$ as a function of frequency ω for a classical two-component plasma at solar core conditions.

With the help of the δ function one integral can be performed, e.g., setting $p'^2=p^2+2m_e\omega/\hbar$. In the limit of high frequencies, an evaluation of Eq. (46) exhibits the same dependence on ω as in the Born approximation, however, with a prefactor depending on density and temperature.

The evaluation of the dynamical collision frequency $\nu^{\rm ladder}(\omega)$ in the approximation Eq. (46) is shown in Fig. 10 for solar core conditions. It is compared with the treatment in the first Born approximation. While the overall dependence on the frequency is similar, the approximations differ in the magnitude. Taking into account strong collisions can lead to collision frequencies up to 15% higher than the Born approximation if the frequency is in the vicinity of the plasma frequency.

IV. DISCUSSION OF CONVERGENCE PROPERTIES

A. Dynamically screened binary collision approximation

To give a consistent description of the effect of collisions in a Coulomb system, we have to combine dynamical screening and strong collisions. Up to now there is no solution available for the dynamically screened ladder approximation in order to calculate a frequency-dependent collision term in a one-moment approach which shall be called $\nu^{(P_0)}(\omega)$. An approximation for the static limit, which interpolates between weak collisions (small transfer momenta q), which have to be screened dynamically, and strong collisions (large q), where a ladder summation has to be performed, has been given by Gould and DeWitt [45]. In this case, a statically screened potential is taken as an interaction for the ladder summation, Eq. (39), which coincides with a Boltzmann collision integral in the kinetic equation, as well as for the lowest-order (Born) collision integral, the static limit of Eq. (26). The latter is subtracted and replaced by a dynamically screened second-order collision integral. A similar approach was applied to the dc conductivity of a fully ionized, nondegenerate hydrogen plasma [42] where the Lenard-Balescu collision integral, Eq. (33), was used.

Thus we construct a dynamical collision frequency which interpolates between the Born approximation with respect to the dynamically screened interaction $\nu^{\rm LB}(\omega)$, Eq. (31), valid

for distant collisions, and the Boltzmann expression, $\nu^{\rm ladder}(\omega)$, Eq. (37), with respect to an effective statical potential, valid for close collisions. To avoid double counting, the collision frequency in the Born approximation $\nu^{\rm Born}(\omega)$, Eq. (26), with respect to the same effective statical potential has to be subtracted,

$$\nu^{(P_0)}(\omega)\approx\nu^{\rm GD}(\omega)=\nu^{\rm ladder}(\omega)-\nu^{\rm Born}(\omega)+\nu^{\rm LB}(\omega). \tag{47}$$

As Fig. 10 shows, the differences between the above approximations are most pronounced in the vicinity of the plasma frequency. The effective potential can be introduced in the low-density limit in such a way that in the zero-frequency limit the collision frequency in the dynamically screened Born approximation coincides with the collision frequency in the Born approximation for the effective interaction, see the introduction of $\kappa_{\rm eff}$ in the preceding section.

Considering the static low-density limit, the different terms coincide to give identical results for $\nu(0)$ in the order $n\ln n$. The differences occur with respect to a factor within the argument of the logarithm, which can be rewritten as a constant (with respect to n) term in addition to $\ln n$. The determination of this constant demands an accurate treatment of dynamically screened binary collisions. As long as we are interested only in the term $\propto n\ln n$, it is sufficient to use the statically screened potential with the Debye screening parameter given above. Then we have $\nu^{(P_0)}(\omega)\approx\nu^{\rm D}(\omega)$,

$$\begin{aligned}\nu^{\rm D}(\omega)&=-i\frac{(2\pi\beta)^{3/2}\hbar^4 n_i e^4}{3m_e^{3/2}\epsilon_0^2}\int\frac{d^3p}{(2\pi)^3}\int\frac{d^3q}{(2\pi)^3}\\&\times\frac{q^2}{(\kappa_D^2+q^2)^2}\,\frac{e^{\beta E^e_{p+q/2}}-e^{\beta E^e_{p-q/2}}}{\Delta E^e_{p,q}-\hbar(\omega+i\eta)}\,\frac{1}{\Delta E^e_{p,q}}\\&=-i\frac{gn_i}{w+i\eta}\int_0^\infty\frac{y^4dy}{(\bar{n}+y^2)^2}\int_{-\infty}^{\infty}dx\,{\rm e}^{-(x-y)^2}\\&\times\frac{1-e^{-4xy}}{xy(xy-w-i\eta)}\end{aligned} \tag{48}$$

with

$$g=\frac{1}{24\sqrt{2}\pi^{5/2}}\,\frac{e^4\beta^{3/2}}{m_e^{1/2}\epsilon_0^2},\quad w=\frac{\hbar\omega}{4k_{\rm B}T},\quad \bar{n}=\frac{\hbar^2\kappa_D^2}{8m_e k_{\rm B}T}. \tag{49}$$

B. Renormalization factor $r(\omega)$

The dynamically screened binary collision approximation $\nu^{(P_0)}(\omega)$ or its extensions obtained by including density effects do not give the correct result for the dynamical conductivity of low-density, nondegenerate plasmas. In particular, the dc conductivity resulting from Eq. (39) contains a prefactor $3/(4\sqrt{2\pi})=0.2992$ which does not coincide with the well-known Spitzer result 0.591 [5]. The correct prefactor is approached if higher moments are taken into account [8,13]. In particular, the inclusion of at least second moments $\vec{P}^c_{k,1}$ in the set of quantum operators, Eq. (17), is important because then electron-electron collisions will contribute to the resistivity. Furthermore, contributions due to the kinetic energy current are taken into account. We will not repeat this derivation but only outline the main aspects.

We restrict ourselves to higher moments of the electron distribution function (adiabatic approximation), Eq. (17), with $c=e$. In analogy to the discussion in Sec. II C, the only contributions to the submatrix elements, Eq. (14), in second order, come from the generalized force-force correlation function

$$\begin{aligned}\langle\dot{\vec{P}}^c_{0,l};\dot{\vec{P}}^{c\prime}_{0,m}\rangle_{\omega+i\eta}&=\hbar^2\sum_{pp'}p_z p_z'(\beta E^c_p)^l(\beta E^c_p)^m\\&\times\lim_{k\to0}\langle v^c_{p,k};v^{c\prime}_{p\prime,k}\rangle^{(2)}_{\omega+i\eta},\end{aligned} \tag{50}$$

see also Eq. (23). We introduce a renormalization factor $r(\omega)$ [46], which relates the n-moment approach of the inverse response function to the one-moment approach

$$r^{(n-1)}(\omega)=\frac{M^{(n)}(0,\omega)}{M^{(1)}(0,\omega)}=\frac{|r_{lm}(\omega)|}{\begin{vmatrix}0 & s_m\\ s_l & r_{lm}(\omega)\end{vmatrix}},$$

$$l,m=0,1,2,\ldots n-1 \tag{51}$$

with

$$s_m=\frac{(\vec{P}^e_{0,0};\vec{P}^e_{0,m})}{(\vec{P}^e_{0,0};\vec{P}^e_{0,0})},\quad r_{lm}=\frac{\langle\dot{\vec{P}}^e_{0,l};\dot{\vec{P}}^e_{0,m}\rangle_{\omega+i\eta}}{\langle\dot{\vec{P}}^e_{0,0};\dot{\vec{P}}^e_{0,0}\rangle_{\omega+i\eta}}. \tag{52}$$

In the nondegenerate limit is

$$s_m=\Gamma(m+\tfrac{5}{2})/\Gamma(\tfrac{5}{2}). \tag{53}$$

In the static limit, the ratios for $r_{nm}(0)$ have been well investigated, see e.g. [8]. The following ratios are obtained if we consider the moments $P^e_{0,0}, P^e_{0,1}$, and $P^e_{0,2}$ in the low-density limit, describing a two-component plasma,

$$r_{00}(0)=1,\quad r_{11}(0)=2+\sqrt{2},$$

$$r_{10}(0)=1,\quad r_{21}(0)=6+11/\sqrt{2},$$

$$r_{20}(0)=2,\quad r_{22}(0)=24+157/\sqrt{8},$$

where terms in $\sqrt{2}$ arise from electron-electron collisions. We obtain the renormalization factors, Eq. (51), $r^{(0)}(0)=1$, $r^{(1)}(0)=0.5176$, $r^{(2)}(0)=0.5123$. The behavior of this series, if further moments in the zero-frequency limit are taken into account, was investigated in [8] and found to converge against the Spitzer value $r_{\rm Sp}(0)=0.2992/0.591=0.5062$. In the case of a Lorentz plasma, where only interaction between electrons and ions is considered, the renormalization factor is $r_{\rm L}(0)=0.2992/1.0159=0.2945$. In that

case, the moment expansion converges more quickly with $r^{(1)}(0)=0.3077$, $r^{(2)}(0)=0.2949$. Subsequently, different prefactors are obtained for the dc conductivity, Eq. (43), or the Brooks-Herring result, see [7].

The frequency-dependent correlation functions of higher moments can be calculated similar to the force-force correlation function, Eq. (A6), with different prefactors in p_z and p_z'. We obtain contributions from electron-ion as well as from electron-electron scattering,

$$\langle \dot{\vec{P}}^{e}_{0,l};\dot{\vec{P}}^{e}_{0,m}\rangle_{\omega+i\eta}=\langle \dot{\vec{P}}^{ei}_{0,l};\dot{\vec{P}}^{ei}_{0,m}\rangle_{\omega+i\eta}+\langle \dot{\vec{P}}^{ee}_{0,l};\dot{\vec{P}}^{ee}_{0,m}\rangle_{\omega+i\eta}. \tag{54}$$

In the Debye approximation, Eq. (48), we find

$$\begin{aligned}\langle \dot{\vec{P}}^{ei}_{0,l};\dot{\vec{P}}^{ei}_{0,m}\rangle_{\omega+i\eta}=&-\frac{i\hbar}{\beta}n_i\Omega_0\frac{n_e\Lambda_e^3}{(2\pi)^6}\frac{e^4}{\epsilon_0^2}\int d^3\vec{p}\int d^3\vec{q}\frac{1}{(\kappa_D^2+q^2)^2}\frac{e^{\beta E^e_{p+q/2}}-e^{\beta E^e_{p-q/2}}}{\Delta E^e_{p,q}-\hbar(\omega+i\eta)}\frac{1}{\Delta E^e_{p,q}}\Bigg[\left(p_z+\frac{q_z}{2}\right)(\beta E^e_{p+q/2})^l\\&-\left(p_z-\frac{q_z}{2}\right)(\beta E^e_{p-q/2})^l\Bigg]\Bigg[\left(p_z+\frac{q_z}{2}\right)(\beta E^e_{p+q/2})^m-\left(p_z-\frac{q_z}{2}\right)(\beta E^e_{p-q/2})^m\Bigg]\\=&-ig\frac{\Omega_0 m_e n_e n_i}{\beta}\int_{-\infty}^{\infty}dx\int_0^{\infty}\frac{y^4dy}{(\bar{n}+y^2)^2}e^{-(x-y)^2}\frac{1-e^{-4xy}}{xy(xy-w-i\eta)}\{x;y\}_{lm}.\end{aligned} \tag{55}$$

The curly brackets stand for polynomials of x and y. For $l=0,1$ we find

$$\begin{aligned}\{x;y\}_{00}&=1,\\ \{x;y\}_{01}&=\{x;y\}_{10}=1+3x^2+y^2,\\ \{x;y\}_{11}&=2+10x^2+9x^4+2y^2+6x^2y^2+y^4.\end{aligned} \tag{56}$$

The contributions due to electron-electron collisions follow as

$$\begin{aligned}\langle \dot{\vec{P}}^{ee}_{0,l};\dot{\vec{P}}^{ee}_{0,m}\rangle_{\omega+i\eta}=&-\frac{i\hbar}{\beta}\frac{4\Omega_0}{(2\pi)^9}\frac{e^4}{\epsilon_0^2}\int d^3\vec{p}\int d^3\vec{p}\,'\int d^3\vec{q}\frac{1}{(\kappa_D^2+q^2)^2}\frac{f^e_{p'+q/2}f^e_{p-q/2}}{\Delta E^e_{p',q}-\Delta E^e_{p,q}}\frac{e^{\beta(\Delta E^e_{p',q}-\Delta E^e_{p,q})}-1}{\hbar z+\Delta E^e_{p',q}-\Delta E^e_{p,q}}\Bigg[\left(p_z+\frac{q_z}{2}\right)(\beta E^e_{p+q/2})^l\\&-\left(p_z-\frac{q_z}{2}\right)(\beta E^e_{p-q/2})^l\Bigg]\Bigg[\left(p_z+\frac{q_z}{2}\right)(\beta E^e_{p+q/2})^m-\left(p_z-\frac{q_z}{2}\right)(\beta E^e_{p-q/2})^m\\&+\left(p_z'-\frac{q_z}{2}\right)(\beta E^e_{p'-q/2})^m-\left(p_z'+\frac{q_z}{2}\right)(\beta E^e_{p'+q/2})^m\Bigg].\end{aligned} \tag{57}$$

The first nonvanishing contribution arises for $l=m=1$,

$$\langle \dot{\vec{P}}^{ee}_{0,1};\dot{\vec{P}}^{ee}_{0,1}\rangle_{\omega+i\eta}=-ig\sqrt{2}\,\frac{\Omega_0 m_e n_e^2}{\beta}\int_{-\infty}^{\infty}dx\int_0^{\infty}\frac{y^4dy}{(2\bar{n}+y^2)^2}e^{-(x-y)^2}\frac{1-e^{-4xy}}{xy(xy-w-i\eta)}\left\{1+\frac{19}{4}x^2\right\}. \tag{58}$$

The real and imaginary part of expressions (55) and (58) have to be considered for an investigation of the frequency-dependent renormalization factor. One integration in the imaginary part can be obtained using the δ function. For the real part a partial fraction decomposition has to be performed,

$$\mathrm{Im}\langle \dot{\vec{P}}^{ei}_{0,l};\dot{\vec{P}}^{ei}_{0,m}\rangle_{\omega+i\eta}=-g\frac{\pi\Omega_0 m_e n_e n_i}{\beta}\frac{1-e^{-4w}}{w}\int_0^{\infty}\frac{2y^3dy}{(\bar{n}+y^2)^2}e^{-(w/y-y)^2}\left\{\frac{w}{y};y\right\}_{lm},$$

$$\mathrm{Im}\langle \dot{\vec{P}}^{ee}_{0,1};\dot{\vec{P}}^{ee}_{0,1}\rangle_{\omega+i\eta}=-g\sqrt{2}\,\frac{\pi\Omega_0 m_e n_e^2}{\beta}\frac{1-e^{-4w}}{w}\int_0^{\infty}\frac{2y^3dy}{(2\bar{n}+y^2)^2}e^{-(w/y-y)^2}\left\{1+\frac{19}{4}\left(\frac{w}{y}\right)^2\right\},$$

$$\mathrm{Re}\langle \dot{\vec{P}}^{ei}_{0,l}; \dot{\vec{P}}^{ei}_{0,m} \rangle_{\omega + i\eta} = -g \frac{\pi \Omega_0 m_e n_e n_i}{\beta} \int_{-\infty}^{\infty} dx\, e^{-x^2} \mathcal{P} \int_0^{\infty} dy \frac{y}{(\bar{n}+y^2)^2} \left[\frac{\{x+y;y\}_{lm}}{xy+y^2-w} \frac{1}{x+y} - \frac{\{x-y;y\}_{lm}}{xy-y^2-w} \frac{1}{x-y} \right],$$

$$\mathrm{Re}\langle \dot{\vec{P}}^{ee}_{0,1}; \dot{\vec{P}}^{ee}_{0,1} \rangle_{\omega + i\eta} = -g\sqrt{2} \frac{\pi \Omega_0 m_e n_e^2}{\beta} \int_{-\infty}^{\infty} dx\, e^{-x^2} \mathcal{P} \int_0^{\infty} dy \frac{y}{(2\bar{n}+y^2)^2} \left[\frac{1+\frac{19}{4}(x+y)^2}{xy+y^2-w} \frac{1}{x+y} - \frac{1+\frac{19}{4}(x-y)^2}{xy-y^2-w} \frac{1}{x-y} \right]. \tag{59}$$

Calculations of the renormalization function $r(\omega)$ as a function of frequency have been performed for a hydrogen plasma at solar core conditions ($\bar{n} = 0.006\,05$). The real and imaginary part of the renormalization factor $r^{(1)}(\omega)$ for a two-moment approach, where in addition to $\vec{P}^{e}_{0,0}$ also $\vec{P}^{e}_{0,1}$ was included, are shown in Fig. 11. The static limit of the real part $r^{(1)}(0) = 0.6166$ depends on the density and converges slowly to the zero-density limit $r^{(1)}_{\mathrm{Sp}}(0) = 0.5176$ when the density is decreased. In the high-frequency limit, higher moments in the generalized linear-response approach can be neglected, and $r(\omega)$ converges to 1. The imaginary part is zero in the static as well as the high-frequency limit. In the intermediate region the renormalization factor is a complex quantity. Besides the electron-ion collisions also the electron-electron collisions contribute, in contrast to the Lorentz model [46].

As a result of the above discussion of the convergence properties of the collision frequency, we obtain the following renormalization of the frequency-dependent conductivity $\sigma(\omega)$ in the long-wavelength limit, Eq. (6):

$$\sigma(\omega) = \frac{\epsilon_0 \omega_{\mathrm{pl}}^2}{-i[\omega + i r(\omega) \nu^{(P_0)}(\omega)]}, \tag{60}$$

where $\nu^{(P_0)}(\omega)$ is the collision frequency calculated in the single moment approach, Eq. (47), within the dynamically screened binary collision appproximation. The renormalization factor $r(\omega)$ takes into account corrections due to higher moments in the set of relevant observables, Eq. (17). In the zero-frequency limit (dc conductivity), results for the statical collision frequency $\nu^{(P_0)}(0)$ as well as for the renormalization factor $r(0)$ are known [7,8,13,42]. The approach given here allows the extension to finite frequencies.

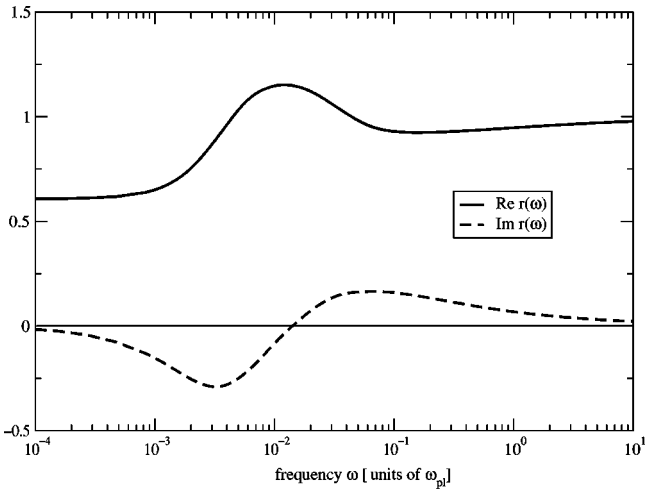

FIG. 11. Renormalization factor $r(\omega)$ as a function of frequency ω for a classical two-component plasma at solar core conditions.

V. CONCLUSIONS

In this work we presented a quantum statistical approach to the dynamical conductivity of low-density fully-ionized plasmas which can be given on the same level as the dc conductivity, in particular in the nondegenerate case. Deviations from the ordinary Drude behavior were obtained for frequencies in the vicinity of the plasma frequency.

To formulate a quantum statistical approach, special attention has been given to a perturbation expansion using the technique of thermodynamic Green functions. Whereas the perturbation expansion of the dielectric function or the polarization function is divergent near the dc limit ($\lim_{\omega\to 0}\lim_{k\to 0}$), the perturbation expansion of the dynamical local-field factor or the dynamical collision frequency is convergent near $\omega = 0$ in the long-wavelength limit.

Partial summations are considered describing screening and strong collisions. In this way, the static limit reproduces the well known results for the dc conductivity. In particular, the summation of ladder diagrams has been performed for the dynamical collision frequency at arbitrary frequencies which leads to expressions containing half off-shell T matrices.

The first-moment sum rules are fulfilled only if the complex character of the dynamical collision frequency is taken into account. This has been shown analytically and numerically. In order to get a convergent third-moment sum rule it is crucial to use a frequency-dependent relaxation time.

Furthermore, a frequency-dependent renormalization factor was introduced which describes the influence of higher moments of the single-particle distribution function, compared with the one-moment approach, within a given perturbation approximation. This way, the discrepancy between ordinary linear-response theory leading, e.g., to the Ziman formula for the dc conductivity for low-density plasmas, and kinetic theory, leading to the Spitzer result, is removed.

In this context, considering the complex dynamical collision frequency $\nu(\omega;T,n)$ as a function of the plasma density n and performing a virial expansion with respect to n, the approximations given in the present paper allow us to determine the correct low-density behavior of $\nu(\omega;T,n)$, which is obtained taking the single-particle distribution as a set of

quantum operators $\{A_l\}$. The inclusion of two-particle correlations into the theory of dc conductivity is also of interest, see [7,12], which leads to a virial expansion for the dynamical local-field factor $G(\vec{k},\omega)$ or the dynamical collision frequency $\nu(\omega)$ if considered as function of the plasma density.

Numerical results were shown for a fully ionized plasma, as it is found for hydrogen at solar core conditions. The results given here should be compared with results from computer simulations. However, quantum statistical simulations for the dynamical conductivity in low-density plasmas are difficult at present.

Using our results for the dielectric function, applications to various measured properties of nonideal plasmas could be considered. E.g., it is possible to calculate the reflectivity of a plasma at a given density and temperature. However, to make the connection to experimentally obtained reflectivities, one has to consider the hydrodynamical expansion of the plasma, e.g., by using density and temperature profiles from a hydrodynamical simulation code. This is beyond the scope of the present paper and will be considered in a forthcoming one. Other applications are experiments measuring the dynamical conductivity of electron-hole plasmas in excited semiconductors, see Ref. [47].

The approach given in this paper relates to weakly coupled, fully ionized plasmas. Improvements are necessary for high-density, strongly degenerated plasmas. In particular, the treatment of the ionic structure factor, the inclusion of local-field factors and the introduction of an effective pseudopotential in order to take into account strong collisions have been discussed in connection with experiments in metal vapors [16,18,22].

The treatment of partially ionized plasmas within the general approach given here has been well investigated in the static limit [8]. The frequency dependence will be the subject of further work. Another direction of future investigation will be the extension of the presented approach to thermoelectric properties, including frequency-dependent thermopower and thermal conductivity. For these quantities, the generalization of the static limit, see [8,13], to finite frequencies should also be possible within our approach to the linear-response theory.

ACKNOWLEDGMENTS

We gratefully acknowledge stimulating discussions with M. Das, A. Hoell, G. Kalman, M.H. Lee, T. Millat, and D. Neilson. One author (H.R.) would like to thank for the hospitality and financial support during a stay at the University of Rostock. Furthermore, we would like to thank the DFG for support within the Schwerpunktprogramm ''Wechselwirkung intensiver Laserstrahlung mit Materie.''

APPENDIX A: EVALUATION OF CORRELATION FUNCTIONS WITH THE GREEN-FUNCTION TECHNIQUE

1. First-order perturbation expansion of $G(\vec{k},\omega)$

The irreducible first-order contributions to the density-density correlation function in Eq. (21) are given by the self-energy and vertex type contributions

$$\begin{aligned}\langle n^c_{p,k};n^{c'}_{p',k}\rangle^{(\mathrm{irred},1)}_{\omega+i\eta}&=\delta_{cc'}\frac{\hbar}{i\beta}\frac{1}{\Delta E^c_{p,k}}\frac{f^c_{p-k/2}-f^c_{p+k/2}}{\Delta E^c_{p,k}-\hbar(\omega+i\eta)}\\&\times\Bigg[-\delta_{pp'}\sum_{p''}V_{cc}(p-p'')\frac{1}{\Delta E^c_{p,k}}\\&\times\frac{f^c_{p''-k/2}-f^c_{p''+k/2}}{\Delta E^c_{p,k}-\hbar(\omega+i\eta)}(2\Delta E^c_{p,k}-\hbar\omega)\\&+V_{cc}(p-p')\frac{1}{\Delta E^c_{p',k}}\frac{f^c_{p'-k/2}-f^c_{p'+k/2}}{\Delta E^c_{p',k}-\hbar(\omega+i\eta)}\\&\times(\Delta E^c_{p,k}+\Delta E^c_{p',k}-\hbar\omega)\Bigg].\end{aligned}\tag{A1}$$

For the current-current correlation function the first-order contribution follows as

$$\begin{aligned}\langle\vec{J}^{\mathrm{el}}_k;\vec{J}^{\mathrm{el}}_k\rangle^{(\mathrm{irred},1)}_{\omega+i\eta}&=-\frac{i}{2}\frac{\omega}{\hbar^4\Omega_0^2\beta k^4}\sum_{pp'c}(m_ce_c)^2(f^c_{p+k/2}-f^c_{p-k/2})\\&\times V_{cc}(\vec{p}-\vec{p}')(f^c_{p'+k/2}-f^c_{p'-k/2})\\&\times\left(\frac{1}{p_z-m_c(\omega+i\eta)/(\hbar k)}-\frac{1}{p'_z-m_c(\omega+i\eta)/(\hbar k)}\right)^2.\end{aligned}\tag{A2}$$

In addition to the first-order contribution of Eq. (18),

$$M^{(\mathrm{irred},1)}(\vec{k},\omega)=\langle\vec{J}^{\mathrm{el}}_k;\vec{J}^{\mathrm{el}}_k\rangle^{(\mathrm{irred},1)}_{\omega+i\eta}/[\langle\vec{J}^{\mathrm{el}}_k;\vec{J}^{\mathrm{el}}_k\rangle^{(0)}_{\omega+i\eta}]^2,\tag{A3}$$

there are further reducible diagrams of first order where the interaction line connects two loops. The latter are immediately evaluated with the result $M^{(\mathrm{red},1)}(\vec{k},\omega)=-i\beta\Omega_0/(\epsilon_0\omega)$. Substituting Eq. (A2) into Eq. (A3), we find within the single-moment approach for the dynamical local-field factor of a two-component system, Eq. (16), the result

$$G^{(1)}(\vec{k},\omega)=i\frac{\epsilon_0\beta\Omega_0k^4}{\omega}[\Pi^{\mathrm{RPA}}(\vec{k},\omega)]^{-2}\langle\vec{J}^{\mathrm{el}}_k;\vec{J}^{\mathrm{el}}_k\rangle^{(\mathrm{irred},1)}_{\omega+i\eta},\tag{A4}$$

see also [25] for the expression of an one-component system. Note that the reducible first-order term is compensated by the 1 in Eq. (16). Thus, the account of only one reducible term $M^{(\mathrm{red},1)}(\vec{k},\omega)$ is equivalent to an infinite partial summation in $\chi(\vec{k},\omega)$ leading to the RPA result.

We add some general expressions which are of use to elaborate also higher-order perturbation expansions. Making use of partial integration and the Kubo identity, we can express the current-current correlation function as

$$\langle\vec{J}^{\mathrm{el}}_k;\vec{J}^{\mathrm{el}}_k\rangle_{\omega+i\eta}=\frac{i}{\omega}(\vec{J}^{\mathrm{el}}_k;\vec{J}^{\mathrm{el}}_k)+\frac{1}{\omega^2}\langle\dot{\vec{J}}^{\mathrm{el}}_k;\dot{\vec{J}}^{\mathrm{el}}_k\rangle_{\omega+i\eta}\tag{A5}$$

by the Kubo scalar product, Eq. (20), and a force-force correlation function. Expressing the time derivative $\dot{\vec{J}}_k^c$ of the particle current operators according to Eq. (22) and applying further partial integrations we have

$$\langle \dot{\vec{J}}_k^c ; \dot{\vec{J}}_k^{c'} \rangle_z = \frac{\hbar^2}{\Omega_0^2} \frac{e_c e_{c'}}{m_c m_{c'}} \sum_{pp'} p_z p_z' \times \Bigg[(\hbar\omega)^2 \frac{\langle v_{p,k}^c ; v_{p,k'}^{c'} \rangle_z}{(\Delta E_{p,k}^c - \hbar z)(\Delta E_{p',k}^{c'} - \hbar z)} - \frac{i}{\hbar} \frac{\Delta E_{p,k}^c \Delta E_{p',k}^{c'}}{\Delta E_{p,k}^c - \hbar z} (n_{p,k}^c ; n_{p',k}^{c'}) - \frac{\Delta E_{p,k}^c}{\Delta E_{p,k}^c - \hbar z} (n_{p,k}^c ; v_{p',k}^{c'}) - \hbar\omega \frac{\Delta E_{p,k}^c}{(\Delta E_{p,k}^c - \hbar z)(\Delta E_{p',k}^{c'} - \hbar z)} (v_{p,k}^c ; n_{p',k}^{c'}) \Bigg]. \tag{A6}$$

In this expression, the first term is explicitly proportional to e^6, thus the correlation function $\langle v_{p,k}^c ; v_{p',k}^{c'} \rangle_z$ itself can be treated at zeroth order to evaluate $\langle \vec{J}_k^{\rm el} ; \vec{J}_k^{\rm el} \rangle_{\omega + i\eta}^{(\rm irred,2)}$. All other terms have to be evaluated within first- or second-order perturbation theory. Because of $\Delta E_{p,k}^c = \hbar p_z k / m_c \propto k$ they do not contribute to the second order in the long-wavelength limit, cf. [7] for the zero-frequency limit.

2. Born approximation

We will show the evaluation of the correlation function $\langle v_{p,k}^c ; v_{p',k}^{c'} \rangle_z$, Eq. (25), using the method of thermodynamic Green functions [38]. The Feynman diagram for the Green function $\mathcal{G}_{vv}(\omega_\mu)$ corresponding to the correlation function according to Eq. (15) was shown in Fig. 1. Different approximations are possible.

In the lowest approximation with respect to the interaction we treat the corresponding four-particle Green function $\mathcal{G}_{vv}(\omega_\mu)$ as a product of four single-particle Green functions, see Fig. 2. We find

$$\begin{aligned} \langle v_{p,k}^c ; v_{p',k}^{c'} \rangle_z^{(2)} = {} & \frac{i}{\hbar\beta} \sum_{plqd} \frac{e^{\beta(\Delta E_{l,q}^d - \Delta E_{\bar{p},k+q}^{\bar{c}}) } - 1}{\hbar z + \Delta E_{l,q}^d - \Delta E_{\bar{p},k+q}^{\bar{c}}} \frac{V_{cd}(q)}{\Delta E_{l,q}^d - \Delta E_{\bar{p},k+q}^{\bar{c}}} \\ & \times f_{l+q/2}^d (1 - f_{l-q/2}^d) f_{\bar{p}-k/2-q/2}^{\bar{c}} \\ & \times (1 - f_{\bar{p}+k/2+q/2}^{\bar{c}}) \{ \delta_{p,\bar{p}+q/2} - \delta_{p,\bar{p}-q/2} \} \\ & \times [V_{cd}(q) \delta_{cc'} \{ \delta_{p',\bar{p}+q/2} - \delta_{p',\bar{p}-q/2} \} \\ & + V_{cd}(q+k) \delta_{dc'} \{ \delta_{p',l-k/2-q/2} \\ & - \delta_{p',l+k/2+q/2} \} + \text{exch. contr.}]. \end{aligned} \tag{A7}$$

Substituting this into Eq. (27) yields in the long-wavelength limit

$$\begin{aligned} \nu^{\rm Born}(\omega) = {} & \frac{i\hbar}{\Omega_0 \epsilon_0 \omega_{\rm pl}^2} \sum_{pp'q,cc'} \frac{e^{\beta(\Delta E_{p',q}^{c'} - \Delta E_{p,q}^c)} - 1}{\hbar(\omega + i\eta) + \Delta E_{p',q}^{c'} - \Delta E_{p,q}^c} \\ & \times \frac{1}{\Delta E_{p',q}^{c'} - \Delta E_{p,q}^c} \left[\frac{e_c^2}{m_c^2} - \frac{e_c e_{c'}}{m_c m_{c'}} \right] \\ & \times q_z^2 V_{cc'}^2(q) f_{p'+q/2}^{c'} (1 - f_{p'-q/2}^{c'}) f_{p-q/2}^c \\ & \times (1 - f_{p+q/2}^c) + \text{exch. contr.} \end{aligned} \tag{A8}$$

Performing the summation over the species leads to expression (26) in Sec. III.

3. Summation of ring diagrams

The summation of ring diagrams leads to the screened interaction, given in Fig. 4. In the following, we shall detail the evaluation of the first diagram only. The contribution to the Green function $\mathcal{G}_{vv}(\omega_\mu)$ from this diagram can be written down with the help of the spectral representation (28) of the screened potential,

$$\begin{aligned} \mathcal{G}_{vv}(\omega_\mu) = {} & -\delta_{cc'} \delta_{pp'} \sum_\lambda \frac{f_{p+k/2+q/2}^c - f_{p-k/2-q/2}^c}{\Delta E_{p,k+q}^c - \hbar\omega_\lambda} \\ & \times V_{cc}(q) \int \frac{d\bar{\omega}}{\pi} \frac{\operatorname{Im} \epsilon^{-1}(q, \bar{\omega} + i0)}{\omega_\lambda + \omega_\mu - \bar{\omega}} \\ = {} & -\delta_{cc'} \delta_{pp'} [f_{p+k/2+q/2}^c - f_{p-k/2-q/2}^c] V_{cc}(q) \\ & \times \int \frac{d(\hbar\bar{\omega})}{\pi} \frac{\operatorname{Im} \epsilon^{-1}(q, \bar{\omega} + i0)}{\Delta E_{p,k+q}^c + \hbar\omega_\mu - \hbar\bar{\omega}} \\ & \times [g(\Delta E_{p,k+q}^c) - g(\hbar\bar{\omega})], \end{aligned} \tag{A9}$$

where $g(E) = [\exp(\beta E - 1)]^{-1}$ is the Bose-Einstein distribution function. After analytical continuation $\omega_\mu \to \omega + i\eta$, the imaginary part of this expression reads

$$\begin{aligned} \operatorname{Im} \mathcal{G}_{vv}(\omega + i\eta) = {} & \delta_{cc'} \delta_{pp'} [f_{p+k/2+q/2}^c - f_{p-k/2-q/2}^c] \\ & \times [g(\Delta E_{p,k+q}^c) - g(\Delta E_{p,k+q}^c + \hbar\omega)] \\ & \times V_{cc}(q) \operatorname{Im} \epsilon^{-1}(q, \Delta E_{p,k+q}^c / \hbar + \omega + i\eta), \end{aligned} \tag{A10}$$

which leads to a contribution to the correlation function $\langle v_{pk}^c ; v_{p'k}^{c'} \rangle_{\omega + i\eta}^{(2,s)}$ according to relation (15). The $\bar{\omega}$ integration can be carried out utilizing the expression (30). In the long-wavelength limit we find

$$\lim_{k\to 0}\langle v^{c}_{pk};v^{c'}_{p'k}\rangle^{(2,LB)}_{\omega+i\eta}$$

$$=\frac{i}{\beta\hbar}\delta_{cc'}\sum_{pp'qc}\frac{V^{2}_{cc}(q)}{|\epsilon_{\mathrm{RPA}}(q,\Delta E^{c}_{p',q}/\hbar)|^{2}}\times\frac{f^{c}_{p'+q/2}-f^{c}_{p'-q/2}}{\hbar(\omega+i\eta)-\Delta E^{c}_{p',q}+\Delta E^{c}_{p,q}}\times\frac{f^{c}_{p+q/2}-f^{c}_{p-q/2}}{\Delta E^{c}_{p',q}-\Delta E^{c}_{p,q}}[g(\Delta E^{c}_{p,q})-g(\Delta E^{c}_{p',q})]\times\{\delta_{p,p+q/2}-\delta_{p,p-q/2}\}\{\delta_{p',p+q/2}-\delta_{p',p-q/2}\}. \quad \text{(A11)}$$

The evaluation of the second diagram does not contribute to the considered density order, see [7]. The third diagram has the same structure as Eq. (A11). It corresponds to the double-exchange term of the Born approximation, see the second term in Eq. (A7). Finally, we find the dynamical collision frequency, Eq. (27),

$$\nu^{\mathrm{LB}}(\omega)=\frac{i}{\hbar\Omega_0\epsilon_0\omega^{2}_{\mathrm{pl}}}\sum_{pp'qcc'}\frac{q_z^{2}V^{2}_{cc'}(q)}{|\epsilon_{\mathrm{RPA}}(q,\Delta E^{c'}_{p',q}/\hbar)|}\times\left[\frac{e_c^{2}}{m_c^{2}}\frac{1}{|\epsilon_{\mathrm{RPA}}(q,\Delta E^{c'}_{p',q}/\hbar)|}-\frac{e_ce_{c'}}{m_cm_{c'}}\times\frac{1}{|\epsilon_{\mathrm{RPA}}(q,\Delta E^{c}_{p,q}/\hbar)|}\right]\frac{f^{c}_{p+q/2}-f^{c}_{p-q/2}}{\hbar(\omega+i\eta)-\Delta E^{c'}_{p',q}+\Delta E^{c}_{p,q}}\times\frac{f^{c'}_{p'+q/2}-f^{c'}_{p'-q/2}}{\Delta E^{c'}_{p',q}-\Delta E^{c}_{p,q}}[g(\Delta E^{c}_{p,q})-g(\Delta E^{c'}_{p',q})], \quad \text{(A12)}$$

where the term proportional to $e_ce_{c'}/(m_cm_{c'})$ originates from the third diagram in Fig. 4. Performing the summation over the species leads to expression (31) in Sec. III A.

4. Summation of ladder diagrams

To describe the effect of strong collisions we perform the summation of ladder diagrams, corresponding to Fig. 9. In the long-wavelength limit the observables $v^{c}_{p,k}$, Eq. (22), shall now be written as

$$v^{c}_{p,0}=\frac{i}{\hbar}\sum_{12}V(1,2)\{\delta_{p,p_2}-\delta_{p,p_1}\}\times\delta_{cc_1}a^{\dagger}_{p_1,c_1}a^{\dagger}_{p'_1,c'_1}a_{p'_2,c'_2}a_{p_2,c_2}, \quad \text{(A13)}$$

where

$$1=(p_1,c_1;p'_1,c'_1)$$

and

$$V(1,2)=V_{c_1c'_1}(|\vec{p}_2-\vec{p}_1|)\,\delta_{c_1c_2}\delta_{c_1,c_2},\delta_{p_2-p_1;p'_1-p'_2}.$$

With $K_p(1)=\delta_{p,p_1}$ for the lowest moment, the analytical expression reads

$$\mathcal{G}_{vv}(\omega_\mu)=\sum_{1234,\omega_\lambda}V(1,2)[K_p(2)-K_p(1)]\times\mathcal{G}_2(1,3;\omega_\lambda+\omega_\mu)V(3,4)[K_{p'}(4)-K_{p'}(3)]\times\mathcal{G}_2(4,2;\omega_\lambda). \quad \text{(A14)}$$

In the low-density limit where $f^{c}_{p}\ll 1$, the two-particle propagator is given in terms of the solution of the two-particle Schrödinger equation, see Sec. III B 1, as

$$\mathcal{G}_2(1,2;\omega_\lambda)=\sum_{nP}\frac{\psi^{*}_{nP}(1)\psi_{nP}(2)}{\omega_\lambda-E_{nP}}. \quad \text{(A15)}$$

Performing in Eq. (A14) the summation over ω_λ, the Bose distribution function occurs. After some straightforward calculations the result (36) is obtained.

We also can express the dynamical collision frequency in terms of the T matrix. We use the operator form and give the representation with respect to the two-particle basis at the end. With the relation

$$\mathcal{G}_2(z)=\int_{-\infty}^{\infty}\frac{d\omega}{\pi}\frac{\mathrm{Im}\,\mathcal{G}_2(\omega+i\eta)}{z-\omega} \quad \text{(A16)}$$

we find

$$\mathcal{G}_{vv}(\omega_\mu)=\int_{-\infty}^{\infty}\frac{d\omega}{\pi}\int_{-\infty}^{\infty}\frac{d\omega'}{\pi}[V,K_p]\mathrm{Im}\,\mathcal{G}_2(\omega+i\eta)\times[V,K_{p'}]\mathrm{Im}\,\mathcal{G}_2(\omega'+i\eta)F(\omega_\mu,\omega,\omega'), \quad \text{(A17)}$$

with

$$F(\omega_\mu,\omega,\omega')=\sum_{\omega_\lambda}\frac{1}{\omega_\lambda+\omega_\mu-\omega}\frac{1}{\omega_\lambda-\omega'}=\frac{e^{\beta(\omega-\omega')}-1}{\omega'+\omega_\mu-\omega}g^{ei}(\omega)[1+g^{ei}(\omega')]. \quad \text{(A18)}$$

Now we utilize the optical theorem

$$\begin{aligned}\mathrm{Im}\ \mathcal{G}_2(\omega+i\eta) &= \frac{-i\eta}{(\omega-H+i\eta)(\omega-H-i\eta)} \\ &= \frac{1}{\omega-H+i\eta}(\omega-H^0+i\eta) \\ &\quad\times\frac{-i\eta}{(\omega-H^0+i\eta)(\omega-H^0-i\eta)} \\ &\quad\times(\omega-H^0-i\eta)\frac{1}{\omega-H-i\eta} \\ &= \mathcal{G}_2^+(\omega)[\mathcal{G}_0^+(\omega)]^{-1}\mathrm{Im}\,\mathcal{G}_0^+(\omega) \\ &\quad\times[\mathcal{G}_0^-(\omega)]^{-1}\mathcal{G}_2^-(\omega) \\ &= V^{-1}T^+(\omega)\mathrm{Im}\,\mathcal{G}_0^+(\omega)T^-(\omega)V^{-1},\end{aligned} \tag{A19}$$

where relations like $V\mathcal{G}_2^{\pm}(\omega)=T^{\pm}(\omega)\mathcal{G}_0^{\pm}(\omega)$ were used. Insertion gives

$$\begin{aligned}\mathcal{G}_{vv}(\omega_\mu) &= \int_{-\infty}^{\infty}\frac{d\omega}{\pi}\int_{-\infty}^{\infty}\frac{d\omega'}{\pi}\mathrm{Im}\,\mathcal{G}_0^+(\omega)T^-(\omega) \\ &\quad\times\left[K_{p'},\frac{1}{V}\right]T^-(\omega')\mathrm{Im}\,\mathcal{G}_0^+(\omega')T^+(\omega') \\ &\quad\times\left[K_p,\frac{1}{V}\right]T^+(\omega)F(\omega_\mu,\omega,\omega').\end{aligned} \tag{A20}$$

With $T^{\pm}(\omega)=V+V\mathcal{G}_0^{\pm}(\omega)T^{\pm}(\omega)=V+T^{\pm}(\omega)\mathcal{G}_0^{\pm}(\omega)V$, we get relations such as $(1/V)T^-(\omega')=1+\mathcal{G}_0^-(\omega')T^-(\omega')$, so that

$$\begin{aligned}&T^-(\omega)\left[K_{p'},\frac{1}{V}\right]T^-(\omega') \\ &\quad= T^-(\omega)K_{p'}-K_{p'}T^-(\omega') \\ &\quad+ T^-(\omega)[K_{p'}\mathcal{G}_0^-(\omega')-\mathcal{G}_0^-(\omega)K_{p'}]T^-(\omega').\end{aligned} \tag{A21}$$

Insertion in Eq. (A20) and representing the operators with respect to a two-particle basis leads to the result (37).

APPENDIX B: HIGH-FREQUENCY BEHAVIOR OF DYNAMICAL CONDUCTIVITY

In this appendix we give details on the determination of the high-frequency behavior $\omega\to\infty$ of the dynamical collision frequency in dynamical screening and in ladder approximation. We start with dynamical screening as given in Eq. (32). Since the real part of the RPA dielectric function is unity in this limit, we obtain $\mathrm{Im}\,\epsilon^{-1}(q,\omega)\approx-\mathrm{Im}\,\epsilon(q,\omega)$. The limiting behavior is the same as for the Born approximation, Eq. (26), and given by

$$\mathrm{Re}\,\nu(\omega)\propto\frac{1}{\omega}\int_0^{\infty}dq\,q^2\,\mathrm{Im}\,\epsilon(q,\omega) \tag{B1}$$

if the q dependence of the Coulomb potential is inserted and the static structure factor is assumed to be $S_i(q)=1$.

In the degenerate limit [$\theta=1/(\beta E_F)\ll 1$], the imaginary part of the dielectric function is [48]

$$\begin{aligned}&\lim_{\theta\to 0}\mathrm{Im}\,\epsilon_{\mathrm{RPA}}(q,\omega) \\ &\quad=\begin{cases} A\hbar\omega/(E_F z^3) & : \quad (u\pm z)^2<1 \\ A(1-(u-z)^2)/z^3 & : \quad (u-z)^2<1<(u+z)^2 \\ 0 & : \quad 1<(u-z)^2,\end{cases}\end{aligned} \tag{B2}$$

using the reduced variables $u=m_e\omega/(\hbar k_F q)$, $z=q/(2k_F)$, $A=(3\pi/128)(\hbar\omega_{\mathrm{pl}}/E_F)^2$. For sufficiently large values of ω, $(u+z)^2$ is always larger than unity. Applying the transformation $q=k_F k$, we are able to perform the q integration in Eq. (B1),

$$\begin{aligned}\int_0^{\infty}dq q^2\ \mathrm{Im}\,\epsilon(q,\omega) &\propto \int_{a-1}^{a+1}\frac{dk}{k}\left[1-\left(\frac{m_e\omega}{\hbar k_F^2 k}-\frac{k}{2}\right)^2\right] \\ &= \left(1+\frac{m_e\omega}{\hbar k_F^2}\right)[\ln(a+1) \\ &\quad-\ln(a-1)]-a, \\ a &= \sqrt{1+\frac{2m_e\omega}{\hbar k_F^2}}.\end{aligned} \tag{B3}$$

The asymptotic form of this expression in the high-frequency limit is proportional to $\omega^{-1/2}$, corresponding to a power law $\omega^{-3/2}$ for $\mathrm{Re}\,\nu(\omega)$.

In the nondegenerate limit ($1/\theta\ll 1$), the imaginary part of the dielectric function is [48]

$$\lim_{1/\theta\to 0}\mathrm{Im}\,\epsilon_{\mathrm{RPA}}(q,\omega)=\frac{\pi\chi_0^2}{8z^3}\theta e^{\beta\mu}[e^{-(u-z)^2/\theta}-e^{-(u+z)^2/\theta}]. \tag{B4}$$

The integration with respect to q, carried out analytically, results in a collision frequency proportional to a modified Bessel function [49]

$$\mathrm{Re}\,\nu(\omega)\propto\frac{1}{\omega}\sinh\left(\frac{\beta\hbar\omega}{2}\right)K_0\left(\frac{\beta\hbar\omega}{2}\right). \tag{B5}$$

The high-frequency limit [49] $K_0(z)\sim\sqrt{\pi/(2z)}e^{-z}(1-1/(8z)+\ldots)$ gives a dependence of $\omega^{-3/2}$ again.

Thus, the asymptotic form of the real part of the collision frequency is given by $\mathrm{Re}\,\nu(\omega)\propto\omega^{-3/2}$ in the degenerate as well as the nondegenerate limit. As a consequence, having in mind that the asymptotic expansion of the dielectric function reads $\epsilon(\omega)=1-\omega_{\mathrm{pl}}^2/\omega^2+i\omega_{\mathrm{pl}}^2\nu(\omega)/\omega^3+0(\omega^{-4})$, we get $\mathrm{Im}\,\epsilon(\omega)\propto\omega^{-9/2}$.

The absorption coefficient $\alpha(\omega)$ for radiation and the imaginary part of the dielectric function are connected via

$$\alpha(\omega)=\frac{\omega}{cn(\omega)}\lim_{q\to 0}\ \mathrm{Im}\,\epsilon(q,\omega), \tag{B6}$$

where c is the speed of light and $n(\omega)$ the index of refraction. Using this relation, the asymptotic scaling of the imaginary part of the dielectric function compares to known results for the frequency dependence of the absorption coefficient of thermal bremsstrahlung at high temperatures [50].

The frequency dependence of the dynamical collision frequency in the ladder approximation can be determined by exploiting the known off-shell behavior of the Coulomb T matrix [51]. Inserting the analytic expression of the half-off-shell T matrix into Eq. (37) results again in a frequency dependence according to $\omega^{-3/2}$.

APPENDIX C: NUMERICAL DETERMINATION OF THE HALF-OFF-SHELL T MATRIX

The Lippmann-Schwinger-equation (38) for the T matrix in partial wave expansion, Eq. (45), is given by

$$T_l(k,k';z)=V_l(k,k')+\frac{1}{2\pi^2}\int_0^\infty dq\,q^2\frac{V_l(k,q)T_l(q,k';z)}{z-q^2}, \tag{C1}$$

where V_l represents the expanded potential. Following [52] we introduce the auxiliary integral equation

$$\Gamma_l(p,k;k^2)=V_l(p,k)+\frac{1}{2\pi^2}\int_0^\infty dq\,q^2A_l(p,q;k^2)\Gamma_l(q,k;k^2), \tag{C2}$$

with the kernel

$$A_l(p,q;k^2)=\frac{V(p,q)-V(p,k)\,\gamma_l(k,q)}{k^2-q^2} \tag{C3}$$

which is nonsingular in contrast to the one in Eq. (C1). The function $\gamma_l(k,q)$ is subject to the condition $\gamma_l(k,k)=1$ and can be chosen to optimize the numerical expense. The integral equation (C2) can be solved by standard techniques for Fredholm equations such as the Nystrom method. The on-shell T matrix is obtained from its solution according to

$$T_l(k,k;k^2)=\frac{\Gamma_l(k,k;k^2)}{1-\frac{1}{2\pi^2}\int_0^\infty dq\,q^2\frac{\gamma_l(k,q)\Gamma_l(q,k;k^2)}{k^2-q^2+i\epsilon}} \tag{C4}$$

and the half-off-shell T matrix using the relation

$$T_l(p,k;k^2)=\frac{\Gamma_l(p,k;k^2)}{\Gamma_l(k,k;k^2)}T_l(k,k;k^2). \tag{C5}$$

[1] H.M. Milchberg, R.R. Freeman, S.C. Davey, and R.M. More, Phys. Rev. Lett. **61**, 2364 (1988).

[2] R. Sauerbrey, J. Fure, S.P. Le Blanc, B. van Wonterghem, U. Teubner, and F.P. Schäfer, Phys. Plasmas **1**, 1635 (1994).

[3] D.F. Price, R.M. More, R.S. Walling, G. Guethlein, R.L. Shepherd, R.E. Stewart, and W.E. White, Phys. Rev. Lett. **75**, 252 (1995).

[4] A.N. Mostovych, K.J. Kearney, J.A. Stamper, and A.J. Schmitt, Phys. Rev. Lett. **66**, 612 (1991).

[5] L. Spitzer, Jr. and R. Härm, Phys. Rev. **89**, 977 (1953); L. Spitzer, Jr., *Physics of Fully Ionized Gases* (Interscience, New York, 1962).

[6] R. Kubo, J. Phys. Soc. Jpn. **12**, 570 (1957); Rep. Prog. Phys. **29**, 255 (1966).

[7] G. Röpke, Phys. Rev. A **38**, 3001 (1988).

[8] H. Reinholz, R. Redmer, and D. Tamme, Contrib. Plasma Phys. **29**, 395 (1989); R. Redmer, H. Reinholz, G. Röpke, R. Winter, F. Noll, and F. Hensel, J. Phys.: Condens. Matter **4**, 1659 (1991); H. Reinholz, R. Redmer, and S. Nagel, Phys. Rev. E **52**, 5368 (1995).

[9] S. Chapman and T.G. Cowling, *The Mathematical Theory of Non-Uniform Gases* (University Press, London, 1952).

[10] H. Grad, in *Handbuch der Physik*, edited by S. Flügge (Springer, Berlin, 1958), Vol. XXII, p. 205.

[11] Yu.L. Klimontovich, *Kinetic Theory of Nonideal Gases and Nonideal Plasmas* (Nauka, Moskow, 1975), in Russian.

[12] A. Esser and G. Röpke, Phys. Rev. E **58**, 2446 (1998).

[13] R. Redmer, Phys. Rep. **282**, 36 (1997).

[14] G. Mahan, *Many-Particle Physics* (Plenum, New York, 1981).

[15] A. Ron and N. Tzoar, Phys. Rev. **131**, 12 (1963); **131**, 1943 (1963).

[16] V.B. Bobrov and S.A. Trigger, Solid State Commun. **56**, 21 (1985).

[17] M.A. Berkovsky and Yu.K. Kurilenkov, Physica A **197**, 676 (1993).

[18] M.A. Berkovsky, Yu.K. Kurilenkov, and H.M. Milchberg, Phys. Lett. A **168**, 416 (1992); M.A. Berkovsky, Physica A **214**, 461 (1995); Yu.K. Kurilenkov, M.A. Berkovsky, S. Hocini, and M.A. Skowronek, J. Phys. B **28**, 2021 (1995).

[19] J.M. Ziman, Philos. Mag. **6**, 1013 (1961); T. E. Faber, *Introduction to the Theory of Liquid Metals* (Cambridge University Press, Cambridge, England, 1972), Chap. 3.

[20] Y.T. Lee and R.M. More, Phys. Fluids **27**, 1973 (1984); G.A. Rinker, Phys. Rev. B **31**, 4207 (1987); F. Perrot and M.W.C. Dharma-wardana, Phys. Rev. A **36**, 238 (1987); W. Ebeling, V. E. Fortov, V. K. Gryaznov, A. Förster, and A. Ya. Polyshchuk, *Thermophysical Properties of Hot Dense Plasmas* (Teubner, Leipzig, 1990).

[21] F. Perrot and M.W.C. Dharma-wardana, Phys. Rev. Lett. **72**, 681 (1994); Int. J. Thermophys. **20**, 1299 (1999).

[22] M.W.C. Dharma-wardana and F. Perrot, Phys. Lett. A **163**, 223 (1992); M.W.C. Dharma-wardana, in *Laser Interactions with Atoms, Solids, and Plasmas*, edited by R. M. More, Vol. 327 of *NATO Advanced Study Institute Series B: Physics* (Plenum, New York, 1992), p. 311.

[23] G. Röpke, Phys. Rev. E **57**, 4673 (1998); G. Röpke and A. Wierling, *ibid.* **57**, 7075 (1998).

[24] H. Reinholz, R. Redmer, G. Röpke, and A. Wierling, Contrib. Plasma Phys. **39**, 77 (1999).

[25] G. Röpke, R. Redmer, A. Wierling, and H. Reinholz, Phys. Rev. E **60**, 2484 (1999).
[26] H. Reinholz, Aust. J. Phys. **53**, 133 (2000)
[27] D.N. Zubarev, V. Morozov, and G. Röpke, *Relaxation and Hydrodynamic Processes*, Vol. 2 of *Statistical Mechanics of Nonequilibrium Processes* (Akademie Verlag/Wiley, Berlin, 1997).
[28] Yu.L. Klimontovich and V.P. Silin, Zh. Éksp. Teor. Fiz. **23**, 151 (1952).
[29] J. Lindhard, K. Dan. Vidensk. Selsk. Mat. Fys. Medd. **28**, 8 (1954).
[30] J. Hubbard, Proc. R. Soc. London, Ser. A **243**, 336 (1957); K. Singwi, M.P. Tosi, R.H. Land, and A. Sjölander, Phys. Rev. **176**, 589 (1968); S. Ichimaru, S. Mitake, S. Tanaka, and X.-Z. Yan, Phys. Rev. A **32**, 1768 (1985); S. Mitake, S. Tanaka, X.-Z. Yan, and S. Ichimaru, *ibid.* **32**, 1775 (1985); R.D. Dandrea, N.W. Ashcroft, and A.E. Carlsson, Phys. Rev. B **34**, 2097 (1986); H.K. Schweng and H.M. Böhm, *ibid.* **48**, 2037 (1993).
[31] C.F. Richardson and N.W. Ashcroft, Phys. Rev. B **50**, 8170 (1994).
[32] J. Hong and M. Howard Lee, Phys. Rev. Lett. **70**, 1972 (1993).
[33] A. Nakano and S. Ichimaru, Phys. Rev. B **39**, 4938 (1989); J. Hong and Y. Shim, J. Phys.: Condens. Matter **5**, 3431 (1993); S.V. Adamian, I.M Tkachenko, J.L. Munoz-Cobo Gonzalez, and G. Verdu Martin, Phys. Rev. E **48**, 2067 (1993); S.V. Adamyan, J. Ortner, and I.M. Tkachenko, Europhys. Lett. **25**, 11 (1994).
[34] G. Kalman and K. Golden, Phys. Rev. A **41**, 5516 (1990).
[35] See *Relaxation and Hydrodynamic Processes* (Ref. [27]), pp. 68–71.
[36] We consider all diagrams corresponding to the perturbation expansion of $\chi(\vec{k},\omega)$, in contrast to $\Pi(\vec{k},\omega)$ where only irreducible diagrams are considered.
[37] The upper index (n) indicates the order in e^2. Since the charge e is already contained in the definition of the currents J_k^{el}, Eq. (12), the expressions $M^{(n)}$, $G^{(n)}$ are of the order $e^{(2n-2)}$, whereas $\langle \vec{J}_k^{\mathrm{el}};\vec{J}_k^{\mathrm{el}}\rangle_{\omega+i\eta}^{(n)}$ is of the order $e^{(2n+2)}$.
[38] W.D. Kraeft, D. Kremp, W. Ebeling, and G. Röpke, *Quantum Statistics of Charged Particle Systems* (Plenum, New York, 1986).
[39] G. Bekefi, *Radiation Processes in Plasmas* (Wiley, New York, 1966).
[40] J.J. Hopfield, Phys. Rev. **139**, A419 (1965).
[41] A. Lenard, Ann. Phys. (N.Y.) **10**, 390 (1960); R. Balescu, Phys. Fluids **3**, 52 (1960); R.L. Gurnsey, *ibid.* **7**, 1600 (1964).
[42] R. Redmer, G. Röpke, F. Morales, and K. Kilimann, Phys. Fluids B **2**, 390 (1990).
[43] D.B. Boercker, F.J. Rogers, and H.E. DeWitt, Phys. Rev. A **25**, 1623 (1982).
[44] J. Dawson and C. Oberman, Phys. Fluids **5**, 517 (1962).
[45] J. Hubbard, Proc. R. Soc. London, Ser. A **262**, 371 (1961); H.A. Gould and H.E. DeWitt, Phys. Rev. **155**, 68 (1967).
[46] H. Reinholz and G. Röpke, in *Condensed Matter Theories*, edited by g. A. Anagnostatos and R. F. Bishop (Nova Science, New York, 2000), Vol. 15.
[47] B.E. Sernelius, Phys. Rev. B **36**, 1080 (1987); **40**, 12 438 (1989); **43**, 7136 (1991).
[48] N.R. Arista and W. Brandt, Phys. Rev. A **29**, 1471 (1984); N. Iwamoto, *ibid.* **30**, 3289 (1984).
[49] *Handbook of Mathematical Functions*, edited by M. Abramowitz and I.A. Stegun (Dover, New York, 1972).
[50] W.J. Karzas and R. Latter, Astrophys. J., Suppl. **6**, 167 (1961).
[51] H. van Haeringen, L.P. Kok, and J.W. de Maag, Phys. Rev. A **32**, 677 (1985).
[52] K.L. Kowalski, Phys. Rev. Lett. **15**, 798 (1965); S.K. Adhikari, Phys. Rev. C **19**, 1729 (1979).